

2007

Survey of small unmanned aerial vehicle electric propulsion system

Edward Kenneth Corrigan
University of Dayton

Follow this and additional works at: https://ecommons.udayton.edu/graduate_theses

Recommended Citation

Corrigan, Edward Kenneth, "Survey of small unmanned aerial vehicle electric propulsion system" (2007).
Graduate Theses and Dissertations. 2123.
https://ecommons.udayton.edu/graduate_theses/2123

This Thesis is brought to you for free and open access by the Theses and Dissertations at eCommons. It has been accepted for inclusion in Graduate Theses and Dissertations by an authorized administrator of eCommons. For more information, please contact mschlangen1@udayton.edu, ecommons@udayton.edu.

SURVEY OF SMALL UNMANNED AERIAL VEHICLE ELECTRIC PROPULSION SYSTEM

Thesis

Submitted to

The School of Engineering of the
UNIVERSITY OF DAYTON

in Partial Fulfillment of the Requirements for

The Degree

Master of Science in Aerospace Engineering

by

Edward Kenneth Corrigan IV

UNIVERSITY OF DAYTON

Dayton, OH

December, 2007

SURVEY OF SMALL UNMANNED AERIAL VEHICLE ELECTRIC PROPULSION SYSTEM

APPROVED BY:

Aaron Altman, Ph.D.
Advisory Committee Chairman
Assistant Professor, Department of
Mechanical and Aerospace
Engineering

Kevin P. Halfinan, Ph.D.
Committee Member
Chairperson, Department of
Mechanical and Aerospace
Engineering

John Petrykowski, Ph.D.
Committee Member
Associate Professor, Department of
Mechanical and Aerospace
Engineering

Malcolm W. Daniels, Ph.D.
Associate Dean
School of Engineering

Joseph E. Saliba, Ph.D.
Dean, School of Engineering

ABSTRACT

SURVEY OF SMALL UNMANNED AERIAL VEHICLE ELECTRIC PROPULSION SYSTEM

Name: Corrigan, Edward, Kenneth
University of Dayton

Advisor: Dr. Aaron Altman

The major driving force behind Small Unmanned Aerial Vehicle (SUAV) development is the need for longer endurance. The United States Military wants platforms that can maintain functional flight for hours and even days. In order to more fully understand the design space and the factors that affect the endurance of an aircraft, a great deal of technical information needs to be available about the weight and aerodynamics of the aircraft in general. Equally as important, yet often neglected however, is information on the propulsion source. Most SUAVs today use commercial off of the shelf (COTS) technology that generally has been used in the hobby model airplane arena. Lack of accurate engine/motor data prevents designers from using a traditional conceptual design approach. The endurance times of these flights are estimates at best and actual endurance times are not calculated. Few motors on this scale have been evaluated for such things as efficiency, power, and torque. This effort evaluated three electric motors ranging from 0.25 hp to 0.8 hp in a wind tunnel test section under various throttle settings and airspeeds. Thrust, torque, RPM, current, and voltage were measured. This data were then

used to calculate efficiency for each system at various throttle settings. Significant wind tunnel test section blockage occurred under some of the throttle setting and wind speed combinations. Wall surface static pressure measurements were then recorded in order to accurately correct for blockage. After the corrections were made the most efficient operating conditions were reported and analyzed for each motor tested, as identification of these optimal conditions offer the greatest enhancement to endurance from the standpoint of electric motor propulsion.

ACKNOWLEDGMENTS

First and foremost I would like to thank my advisor Dr. Aaron Altman for all of his mentorship and support. Without his passion for engineering, experimenting, and most of all teaching, I am sure this effort would not have been completed. I am also honored at the level of priority I felt in Dr. Altman's life during this endeavor, as he is an important man that is always being pulled in numerous different directions. Thank you sir, for all of your help and advice along the way.

I would also like to thank Mr. Cameron Riepenhoff of Wright Patterson Air Force Base for offering his assistance in the preparation of the experiment. Not only did he help me prepare most of the instrumentation that was used, he also offered his extensive knowledge of experimenting in order to make sure I had the best chance at success. Thanks Cam, I couldn't have done it without you.

I would also like to thank the employees of Green Machine, Machining Company in Dayton Ohio for their contributions. They generously donated their time and materials to machine one of the motor mounts for the experiment. Thanks for all your help guys.

Last, I would like to thank my good friend Lt Chris De La Pena for his help in running the extremely large numbers of test run iterations. Without him this effort could have

taken a lot longer than it did. As Chris and I always joked about, “Four hands are often better than two”. Thanks again man!

TABLE OF CONTENTS

ABSTRACT	iii
ACKNOWLEDGMENTS.....	v
INTRODUCTION	1
LITERATURE SEARCH	3
BACKGROUND.....	13
EXPERIMENTAL SETUP	17
RESULTS	26
B20-18L	26
B40-10S	27
B40-10L	27
Additional Correction Methods	28
B20-18L	39
B40-10S	49
B40-10L	60
Experimental Error and Uncertainty	69
Motor Comparison	70
B20-18L and B40-10S	71
B40-10S and B40-10L	74
CONCLUSIONS	78
FUTURE RESEARCH.....	81
APPENDIX A.....	83
BIBLIOGRAPHY	92

TABLE OF CONTENTS

ABSTRACT	iii
ACKNOWLEDGMENTS	v
INTRODUCTION	1
LITERATURE SEARCH	3
BACKGROUND	13
EXPERIMENTAL SETUP	17
RESULTS	26
B20-18L	26
B40-10S	27
B40-10L	27
Additional Correction Methods	28
B20-18L	39
B40-10S	49
B40-10L	60
Experimental Error and Uncertainty	69
Motor Comparison	70
B20-18L and B40-10S	71
B40-10S and B40-10L	74
CONCLUSIONS	78
FUTURE RESEARCH	81
APPENDIX A	83
BIBLIOGRAPHY	92

LIST OF FIGURES

Figure 1 - Accelerated flow in a wind tunnel	14
Figure 2 - Instrument Base Configuration	18
Figure 3 - Electric Motor Instrumentation Configuration (side view).....	19
Figure 4 - Motor Integration (top view).....	19
Figure 5 - Throttle Controlling Servo Tester	21
Figure 6 - Medusa Research's Power Analyzer Pro.....	22
Figure 7 - Unistrut Test Stand mounted in Wind Tunnel	25
Figure 8 - Point Source Theory in Wind Tunnel	29
Figure 9 - Pressure Tap Close Up	30
Figure 10 - B20-18L Velocity Profile at 10 mph.....	31
Figure 11 - B20-18L Velocity Profile at 20 mph.....	32
Figure 12 - B20-18L Velocity Profile at 35 mph.....	32
Figure 13 - B40-10S Velocity Profile at 20 mph.....	33
Figure 14 - B40-10S Velocity Profile at 35 mph.....	33
Figure 15 - B40-10S Velocity Profile at 50 mph.....	34
Figure 16 - B40-10L Velocity Profile at 25 mph.....	34
Figure 17 - B40-10L Velocity Profile at 40 mph.....	35
Figure 18 - B40-10L Velocity Profile at 55 mph.....	35

Figure 19 - Hackett, Wilsden, and Lilley's Asymptote Description	36
Figure 20 - B20-18L at 10 mph Correction Comparison.....	40
Figure 21 - B20-18L Efficiency Comparison at 10 mph	40
Figure 22 - B20-18L Thrust Horsepower Comparison at 20 mph.....	43
Figure 23 - B20-18L Efficiency Comparison at 20 mph	43
Figure 24 - B20-18L Thrust Horsepower Comparison at 35 mph.....	46
Figure 25 - B20-18L Efficiency Comparison at 35 mph	46
Figure 26 - B20-18L Thrust Coefficient vs Advance Ratio Plot.....	47
Figure 27 - B40-10S Thrust Horsepower Comparison at 20 mph	50
Figure 28 - B40-10S Efficiency Comparison at 20 mph	50
Figure 29 - B40-10S Thrust Horsepower Comparison at 35 mph.....	53
Figure 30 - B40-10S Efficiency Comparison at 35 mph	53
Figure 31 - B40-10S Thrust Horsepower Comparison at 50 mph.....	57
Figure 32 - B40-10S Efficiency Comparison at 50 mph	57
Figure 33 - B40-10S Thrust Coefficient vs Advance Ratio Plot	58
Figure 34 - B40-10L Thrust Horsepower Comparison at 25 mph.....	61
Figure 35 - B40-10L Efficiency Comparison at 25 mph	61
Figure 36 - B40-10L Thrust Horsepower Comparison at 40 mph.....	64
Figure 37 - B40-10L Efficiency Comparison at 40 mph	64
Figure 38 - B40-10L Thrust Horsepower Comparison at 55 mph.....	67
Figure 39 - B40-10L Efficiency Comparison at 55 mph	67
Figure 40 - B40-10L Thrust Coefficient vs Advance Ratio Plot.....	68
Figure 41 - Low Speed B40-10s and B20-18L Efficiency Comparison.....	71

Figure 42 - Mid Speed B40-10S and B20-18L Efficiency Comparison.....	72
Figure 43 - High Speed B40-10S and B20-18L Efficiency Comparison	73
Figure 44 - Low Speed B40 Efficiency Comparison.....	74
Figure 45 - Mid Speed B40 Efficiency Comparison	75
Figure 46 - High Speed B40 Efficiency Comparison	76

LIST OF TABLES

Table 1 - Motor Test Run Matrix.....	23
Table 2 - B20-18L Corrected Data at 10 mph	39
Table 3 - B20-18L Corrected Data at 20 mph	42
Table 4 - B20-18L Corrected Data at 35 mph	45
Table 5 - B40-10S Corrected Data at 20 mph.....	49
Table 6 - B40-10S Corrected Data at 35 mph.....	52
Table 7 - B40-10S Corrected Data at 50 mph.....	56
Table 8 - B40-10L Corrected Data at 25 mph	60
Table 9 - B40-10L Corrected Data at 40 mph	63
Table 10 - B40-10L Corrected Data at 55 mph	66
Table 11 - Motor Maximum Power and Efficiency for Corrected Hackett Values.....	77
Table 12 - B20-18L Uncorrected Data at 10 mph	83
Table 13 - B20-18L at 20 mph.....	83
Table 14 - B20-18L at 35 mph.....	84
Table 15 - B40-10S at 20 mph.....	84
Table 16 - B40-10S at 35 mph.....	85
Table 17 - B40-10S at 50 mph.....	85
Table 18 - B40-10L at 25 mph.....	86
Table 19 - B40-10L at 40 mph.....	86

Table 20 - B40-10L at 55 mph.....	87
Table 21 - B20-18L Drag Correction Numbers.....	87
Table 22 - B40-10S Drag Correction Numbers	88
Table 23 - B40-10L Drag Correction Numbers.....	88
Table 24 - Pressure Tap Locations in Test Section.....	89
Table 25 - B20-18L Error at 10 mph	89
Table 26 - B20-18L Error at 20 mph	89
Table 27 - B20-18L Error at 35 mph	89
Table 28 - B40-10S Error at 20 mph	90
Table 29 - B40-10S Error at 35 mph	90
Table 30 - B40-10S Error at 50 mph	90
Table 31 - B40-10L Error at 25 mph	90
Table 32 - B40-10L Error at 40 mph	90
Table 33 - B40-10L Error at 55 mph	91

LIST OF SYMBOLS

α_1	calculated variable in Glauert correction
A	propeller disk plane area, ft^2
A_5	calculated variable in Hackett correction
AHr_{BATT}	amp hour rating of battery, AHr
$Amps_{TOTAL}$	total amps drawn by motor
b	longitudinal length of wind tunnel test section
BHP	brake horsepower, hp
C	wind tunnel test section cross-sectional area, ft^2
C_D	coefficient of drag
C_L	coefficient of lift
$C_{P_{EMPTY}}$	coefficient of pressure for empty wind tunnel
$C_{P_{POWERED}}$	coefficient of pressure under powered test run
D	drag, lbs
D_{Length}	propeller diameter, feet
η	internal combustion engine efficiency
η_{PROP}	propeller efficiency
η_{TOTAL}	propulsive efficiency
I	current, Amps
J	advance ratio
L	lift, lbs
n	propeller rotational rate, RPM
P_{IN}	power into motor, hp
Q	torque, ft-lbs
Q_w	source strength, ft^3/s
ρ	air density, $\frac{lb \cdot s^2}{ft^4}$
σ	air density ratio, density at altitude to sea level density
S	wind area, ft^2

SFC	specific fuel consumption, $\frac{lb}{hp \cdot hr}$
τ_4	variable calculated for Glauert correction
T	thrust, lbs
t_{END}	endurance time, hours
THP	thrust horsepower, hp
U_∞	free-stream velocity, Hackett notation, $\frac{ft}{s}$
$\frac{\Delta u}{U_\infty}$	dimensionless velocity change, Hackett correction
$\left(\frac{\Delta u}{U_\infty} \right)_{MIN}$	minimum velocity change for Hackett correction
V	free-stream velocity, standard notation, $\frac{ft}{s}$
V'	corrected free-stream velocity, Glauert correction
$\frac{ft}{s}$	
V_E	electric potential, Volts
W	aircraft weight, lbs
W_f	final aircraft weight, lbs
W_i	initial aircraft weight, lbs
x/b	x longitudinal test section position normalized by test section length

INTRODUCTION

In the world of aircraft design most engineers and pilots alike find it valuable to know various flight characteristics like range, endurance, and gross takeoff weight, just to name a few. These are very important parameters that are unique to each separate aircraft and are even mission specific in most cases. The heavier the aircraft is at take off the more fuel it will need to takeoff, the longer the runway will need to be, and the shorter the endurance and range will be. These factors are considered on a daily basis in both military and civilian situations. When talking about unmanned aerial vehicles (UAV) the situation is not the same.

The term UAV can be used to describe any air platform from the extremely large Global Hawk to very small systems that fit in the palm of your hand. The term UAV is not limited to only military applications; it also includes model airplanes that have been flown for decades. It is this class of UAV known as small UAVs (SUAVs) that are being utilized by Marines, Air Force Security Forces, Navy personnel, and Army Soldiers. These hand launched SUAVs are used by our military on a daily basis all over the world and are based heavily on the same technology hobbyists use in their model airplanes. The same electric motors, batteries, and in some cases gas engines are used by both government and civilian alike. Unlike the larger military and civilian aircraft, the necessary parameters for SUAVs are not known to accurately determine important factors such as range and endurance. A recent push by military leadership has put

endurance as the main driving force behind SUAV mission design and employment.

Since the same commercial off of the shelf (COTS) propulsion systems are used by the military and civilian world, the military has looked to the civilian manufacturers for the necessary data to determine the endurance of these SUAVs. The problem lies in the fact that modelers do not care about long endurances. They fill their fuel tanks, charge their batteries and have an hour or so worth of flight time which fits their needs perfectly. No one has wanted nor needed to evaluate SUAV sized propulsion systems to determine the necessary factors for an aircraft's endurance calculation.

The UAV is not a fad of the present that will fade off to other technologies. It is a force enabler that removes human constraints on aircraft performance and offers battlefield commanders one more capability to fight a war. The day will come where a SUAV is launched and can fly and monitor the battlefield for days and not minutes. This can only be achieved with the necessary research and development of a smaller class of propulsion systems that has not yet been initiated.

LITERATURE SEARCH

This particular thesis topic was chosen because the knowledge it would provide would be very useful to modelers and engineers alike. The endurance and efficiency information for SUAV propulsion systems have not been well documented and in most cases were considered irrelevant. Research and reports in this area are also very scarce and this was proven based on the results of the literature search. Seven total papers were found that directly applied to this area of study with some being more applicable than others but are all still worth being mentioned.

In February of 2003 an Army Phase I small business innovative research project (SBIR) titled Small, Heavy Fuel, Compression Ignition Small UAV Engines. The research effort itself was focused on the development of low fuel consumption UAV engines. The contract was sponsored by DARPA and was a feasibility study into the development of a heavy fueled opposing piston opposing cylinder (OPOC) engine. This type of engine was hypothesized to cut down on the friction cause by the rod pushing the piston head against the cylinder wall by having the two cylinders directly opposite each other. A two cylinder model was predicted based on computer code to have a 9 hp power rating. These two cylinders could also be stacked up to six giving an effective power rating of 35.4 hp. Most of the paper discussed the feasibility of designing and successfully fabricating an engine that could in fact run on heavy fuel, have low fuel consumption,

and be much more efficient than standard engines of the time. In order to complete this analysis engines from various manufacturers were evaluated in order to see where the benchmark stood in commercial products. The engines were split up into two groups for comparison purposes. The groups were designated by the engine stroke which both 2 and 4 stroke engines. Various parameters were reported such as bore, stroke, displacement, power, mean piston speed, torque, weight, and power density. The means by which these evaluations were completed was not reported, only the results were listed. The claim was that the two stroke engine configuration was the best and offered double the power density, 40% more power, 35% higher engine speed, and 20% lower engine weight. There was no evidence or report of a follow up Phase II. The numbers of some of the benchmarked engines have the ability to be verified here.

The next paper was titled Stealthy, Efficient, Light-weight, JP-8 Fueled Hybrid Electric Propulsion systems for UAVs. This was a SBIR Phase II contract sponsored by DARPA but managed by the Army. This effort researched the optimum configuration of a SUAV propulsion system. It evaluated the use of a JP-8 fueled engine hybridized with an electric motor and battery. The system was capable of running in the high power all internal combustion engine mode, hybrid engine/electric mode, and stealthy all electric mode. The main drive of the hybridized engine was to have the capability of starting and stopping the engine as desired while still having the battery to run the intelligence, surveillance, and reconnaissance (ISR) sensors. The research effort looked heavily at which configuration would allow for the largest takeoff weight and largest allowable payload weight. Aside from the operating configuration the contract also looked at

different drive train systems and their effect on the desired outcome of the SUAV design. These variations were direct, differential, ring motor, and pure battery with charger in field.

The report also analyzed various custom built motors for the contract as well as COTS motors to see which was the most power dense. The same was done for numerous gas engines to see which models performed better and offered the most power per unit weight. They went into great detail about the pros and cons of the various small engine designs and described why they have poor performance. Specific fuel consumption (SFC) and power data for numerous small engines was also listed. The author had diesel, gasoline, glow fuel, and turbine engines displayed but with no mention of the methods used to retrieve this data or what the specific models of the engines were. Turbochargers were also looked at as a viable way to increase the gross takeoff of the SUAV. The turbochargers were analyzed based on the added power each brought to the system along with each respective weight penalty.

Most of the analysis however was centered around a JP-8 capable diesel that was developed in Phase I of the contract. SFC data for this engine hybridized with the electric motor and battery was listed in the report. Discrepancies were noted in the fact that the SFC was constant over the thrust envelope for the propulsion system which is counterintuitive. It was also not clear as to whether the engine was running alone or if the hybrid system was engaged as well. This is unclear because the report spoke of various operating modes for the system.

There was also a quarterly report entitled Engine Evaluation and Optimization and seemed extremely relevant. All effort was made to contact both the government office and the contractor to receive the final report. This search ended with no success of finding the final report. However, the SBIR Phase II quarterly report still had some relevant information in it.

The report discussed efforts to develop gasoline and heavy fueled engines for the Silver Fox UAV. Reliability was the primary objective in their design and development. This seemed to be most easily achieved with already developed gas engines and not the hard fuel converted engines. Their first effort was to use a 21cc Echo 2-cycle string trimmer engine. This was done because the Echo was the smallest available gasoline engine out on the market. Their other concurrent effort was to adapt the OS 91 SII and 120 SIII to gasoline fuel from their designed fuel of glow fuel.

The contractor also evaluated an RCS 140 engine that was shown to operate the same on gasoline as it did on heavy fuels. The paper gave fuel consumption data as a function of engine RPM for the 140 along with propeller and power information. The researchers also developed and tested an electric pre-heating system to help vaporize the fuel to enable it to start up more easily. It consisted of a diesel glow plug that was used to heat the combustion chamber. The ambient temperature was stated to be 85 degrees F and with 2 minutes pre-heating was able to start in 20 seconds and with 3 minutes of pre-heat and an adjusted carburetor, started in 6 seconds.

As for the 21cc gasoline engine, it was evaluated to produce less thrust than the OS FS-91SII that was normally used. The 21cc trimmer engine was suspected of being faulty and was replaced. The new engine offered significantly more power. The glow OS FS-120SIII and OS FS-91SII were in the process of being converted to gasoline operation by the fabrication of the needed carburetors and accessories. This was all the quarterly report covered and would have been more useful had a final report been found.

The next paper was another SBIR Phase II that was evaluating a specific class of engines that were in the 3.5-5 hp range. The topic was in direct support of the development of the Area Dominator munition and was centered toward its design requirements. Different types of heavy fueled engines were compared to see which offered the best performance with respect to mission endurance. This meant that the specific fuel consumption was to be at a minimum. Data was recorded using an RC engine dynamometer in standard atmosphere conditions with no utilization of a wind tunnel making the data static and quite different from what could be expected in an operational situation. Fuel consumptions were compared as a function of total load for compression and spark ignition engines. Two and four stroke models were also compared to see which was more effective for the Area Dominator application. The paper also went into discussion for the start and re-start capability of the propulsion system and the need for a motor/generator to do this. This was not talked of as a hybrid propulsion source but as a starter much like automobiles use. This topic only looked at one size of engine and not various sizes or even different types of propulsion like electric or hybrid electric. The

specific fuel consumption and power analysis was also conducted in a static environment without the use of a wind tunnel making it very different from the efforts of this thesis. The Army Research Laboratories Unmanned Aerial Vehicle Comparison Study written in April of 2005, conducted an extensive UAV sizing study for three different UAV platforms. Each of the three platforms was then customized in 16 different configurations to be tested against various mission scenarios. The varied aspects of each configuration were the propulsion system and payload weight. The different propulsion systems were gasoline based engines, diesel based engines, alcohol based engines, and electric motors. The added payload weight translated into more allowable fuel for the mission. These 16 different UAV configurations were then put through identical mission scenarios to see which configurations performed better than others. Each mission scenario varied by range of the mission as well as loiter time on target. Graphs were presented to tell how each UAV configuration performed for each scenario and what payload weight allowed a roundtrip mission success, one way success, or no success what so ever. Average fuel consumptions for each configuration was also reported but was not clear as to how it was recorded or under what flight or power conditions it was recorded under. This effort conducted a very interesting and extensive sizing study for UAVs under various conditions and their ability to complete various lengths of missions. Fuel consumption data were sparse and not very well explained.

The Department of energy funded a SBIR Phase II contract that concluded in 1999 dealing with the development of a small, lightweight, efficient engine for SUAVs. Specifically it was designed for the Aerosonde UAV that gathers weather data over the

Atlantic. Endurance is important in the use of the Aerosonde, so a highly efficient engine was necessary to enable longer mission profiles. Most of the development effort was in the actual design of the engine and offered little comparison to other propulsion sources that are currently being utilized by UAV designers. The designers, The Insitu Group, claimed that the designed engine could achieve a specific fuel consumption of less than $0.49 \frac{lb}{hp \cdot hr}$ at sea level and exactly $0.49 \frac{lb}{hp \cdot hr}$ at cruising altitude. The paper presented a few graphs with numerous fuel consumption curves plotted on the same power/RPM graph. The manner that this engine was evaluated was not made clear and the methods used were not described at all and left no room to duplicate this effort. Only one engine was evaluated for a specific purpose and not compared against other models or propulsion sources. The paper did not even focus as much on the evaluation of the engine as it did on its mechanical design and construction, leaving much room for more engine evaluation and comparison.

The most applicable resource that was found was a thesis written at the Naval Postgraduate School in Monterey California entitled Development of a Flight Test Methodology for a U.S. Navy Half-Scale Unmanned Air Vehicle. The thesis was published in March of 1989, right at the start of the heightened military interest in UAVs and the beginning of the Navy's UAV program. At that point, design studies of various UAV configurations had just began evaluating each for various levels of effectiveness. The idea of the thesis was that before new designs could be implemented or UAVs used as a test bed for other applications, their performance needed to be predictable and have the ability to be modeled. The thesis developed a test methodology that used ground

evaluations in a wind tunnel and compared that data with actual flight test information. The two were combined and compared to develop an accurate performance analysis of the given UAV design.

The Naval Postgraduate School's vertical low speed wind tunnel was used for all ground tests. It was a subsonic, single return, closed circuit tunnel with a test section 3.5 ft by 5 ft which was octagon shaped. The test matrix consisted of recording engine torque, RPM, and thrust for an electric motor and internal combustion engine to get power data along with propeller efficiency. The torque was measured using a simple lever arm calculation. The torque from the engine mounted to a stand was transferred to the lever arm that pressed down on a calibrated scale. The force on the scale and the length of the lever arm gave the torque of the engine at various throttle settings and with various propellers. The RPM was measured using a magnetic transducer to record the 0.5 Volt saw tooth electrical signal generated by the rotation of the 30 tooth pick-up wheel. This was output on a digital tachometer for visual recording as well. The thrust was recorded using strain gauges attached to a beam. The strain gauges measured the amount of deflection of the beam under loads and output a voltage. Each strain gauge was verified using a strain indicator and the calibration curve obtained by applying known loads to the beam and recording the output voltage, measured on a multimeter. RPM was measured concurrently with both the torque stand measurements and the thrust measurements in the wind tunnel. Graphs of Power (SBHP) versus RPM were produced along with effective thrust versus RPM with numerous curves for each throttle setting. This wind tunnel data

was then used to calculate the effective thrust coefficient and was plotted against the advance ratio.

This paper presented a foundation for UAV evaluation and performance prediction with many areas of interest, such as endurance, left without analysis. Fuel consumption data for each propulsion source and current for the motor were not measured at all leaving a level of efficiency unknown. One engine was compared to one motor and not across numerous sizes to see how each would perform for each class of UAV. This leaves a lot of room for improvement in both specific fuel consumption analysis and engine/motor size analysis.

Wind Tunnel Blockage

It was assumed that wall corrections would be needed in order to correct for the fact that the test would not be performed in truly freestream conditions. Two methods would be utilized to correct the data and compared. Glauert's velocity correction method described in the background section, and the second was found in a paper titled Estimation of Tunnel Blockage from Wall Pressure Signatures: A Review and Data Correlation by Hackett, Wilsden, and Lilley. This paper described in detail the method of correcting wind tunnel drag readings based on wall static pressure measurements. From the wall static pressures, pressure coefficients could be calculated and then used to determine a normalized velocity change at each of the static pressure ports. This value $\frac{\Delta u}{U_{\infty}}$ was then

used to establish a horizontal buoyancy correction on the force measurements that were taken. This correction would help alleviate the artificial thrust that was being recorded, and if left uncorrected would invalidate the data.

The second of the two blockage correction references was a Master's thesis from the University of Maryland titled Wind Tunnel Blockage Corrections for Propellers written by Ryan Fitzgerald. This thesis took into account most methods that have been established for correcting for blockage in a wind tunnel environment. The author went on to focus on the correction of motor driven propellers in two wind tunnels with different sized test sections and how some of the blockage correction theories were not applicable to a rotating propeller. The methods that the author focused on were the ones described above in Hackett, Wilsden, and Lilley's paper as well as a more recent publication by Sorensen and Mikkelsen published in 2002. The focus of the paper was not on the correction of the force itself, but a correction of the velocity that the disk plane would be seeing if it were really producing that amount of force. Both methods were checked against each other in this paper. Of the other methods focused on were the Maskell method and a method developed by Ashill and Keating. These were neglected as a possibility as they were not entirely applicable to the situation at hand. They dealt with bluff body corrections in a wind tunnel such as cars and flat plates, and not rotating propeller planes that actually passed some free-stream air through them. The Sorensen and Mikkelsen Method was also neglected as it required accurate data of the downstream jet diameter in order to correct the velocity. This jet diameter information was not available so the pressure approach was taken.

BACKGROUND

When dealing with aircraft performance, and specifically endurance analysis, certain assumptions need to be made to acquire the necessary equations and to have them in the correct form. The assumption made in this case was that the aircraft would be flying in cruise conditions justifying the use of the relations in Equations 1 and 2.

$$L = W = 0.5\rho V^2 SC_L \quad (1)$$

$$D = T = 0.5\rho V^2 SC_D \quad (2)$$

In cruise conditions the aircraft is not accelerating in any direction, balancing the forces in each direction. This then makes the lift equal to weight as seen in Equation 1 and the drag equal to thrust as seen in Equation 2.

The end result of all of the data is to determine the performance efficiencies of each propulsion system under these test conditions which relates directly to how long an endurance each system might be able to support. To achieve this various values are needed and power is one of them. Equation 3 gives the thrust horsepower (THP) for a given propulsion source.

$$THP = TV \quad (3)$$

The thrust is recorded by the load cell and the freestream velocity will be known and set by the calibrated wind tunnel. It is important though to correct the velocity readings due to effects of the pressure of the walls of the wind tunnel. The increased pressure that builds up behind the propeller disk plane as a function of the disk plane area and tunnel

cross sectional area, produce a greater thrust reading than would normally be achieved. Figure 1 shows flow accelerating around an object in a wind tunnel test section, illustrating the need for the correction.

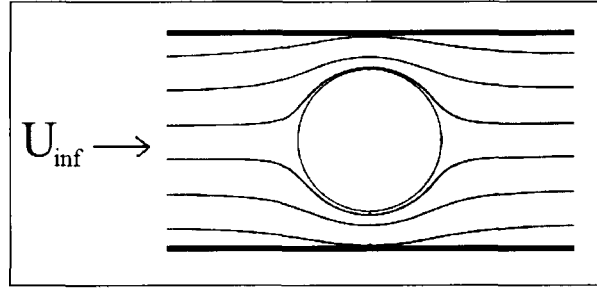


Figure 1 - Accelerated flow in a wind tunnel

Equation 4 corrects for the lack of completely free flow as developed by Glauert.

$$\frac{V'}{V} = 1 - \frac{\tau_4 \alpha_1}{2\sqrt{1 + 2\tau_4}} \quad (4)$$

V' is the corrected velocity and V is the recorded freestream velocity. $\tau_4 = \frac{T}{\rho A V^2}$ with

T being the thrust produced by the propulsion source, ρ being the freestream density,

A representing the propeller disc area, and V being the recorded freestream velocity.

$\alpha_1 = \frac{A}{C}$ is the ratio of propeller disk area A , to the test section cross sectional area C .

This correction makes certain that the thrust recorded corresponds to the accurate freestream velocity. The thrust itself is not adjusted, only the free-stream velocity that thrust would normally be recorded at is corrected. This makes Glauert's method more of a power correction, as the thrust alone is still inaccurate. To have accurate thrust data the wall static pressure correction must be used. This is discussed in greater detail in the Additional Methods section.

Brake horsepower (BHP) is also required to determine the propulsive efficiency of the propulsion system and is given by Equation 5.

$$BHP = \frac{2\pi nQ}{33,000} \quad (5)$$

The BHP requires torque measurements, Q in foot-pounds, as well as the propeller rotational speed measurements, n in rotations per minute (RPM). Knowing both THP and BHP, Equation 6 can be used to calculate the propeller efficiency of the system.

$$\eta_{PROP} = \frac{THP}{BHP} \quad (6)$$

When analyzing the propeller efficiency in Equation 6 it is known to vary by airspeed and propeller rotational speed. These two values are combined into a dimensionless relation known as the advance ratio which is what is most commonly seen being related to propeller efficiency. The advance ratio can be seen in Equation 7.

$$J = \frac{V}{nD_{Length}} \quad (7)$$

Looking at Equation 7, V is the freestream velocity, n is the rotation speed of the propeller, and D_{Length} is the diameter of the propeller. To evaluate the system as a whole, the propulsive efficiency was calculated using thrust horsepower given by Equation 3, and dividing it by the power into the motor. This gives a total system efficiency taking into account the losses from the motor, gearbox, and propeller. This can be seen in Equation 8 and simplifies to thrust times velocity over voltage in multiplied by current in.

$$\eta_{TOTAL} = \frac{THP}{P_{IN}} = \frac{TV}{V_E I} \quad (8)$$

Normally when endurance is discussed it deals with internal combustion engines.

Endurance for these types of propulsions sources is defined by Equation 10.

$$t_{END} = 37.9 \frac{\eta}{SFC} \frac{C_L^{3/2}}{C_D} \sqrt{\frac{\sigma S}{W_i}} \left[\left(\frac{W_i}{W_f} \right)^{1/2} - 1 \right] \quad (10)$$

The efficiency η and specific fuel consumption SFC are factors specific to the propulsion source. The rest of the variables in Equation 10 come from airframe data that is specific to each platform. These values are the lift coefficient C_L , drag coefficient C_D , density ratio σ , wing area S , aircraft initial weight W_i , and the aircraft final weight W_f . This information needs to be known in order to accurately determine the endurance time of the aircraft. When speaking of electric propulsion, as was the case for this effort, the endurance equation reduces greatly. The endurance equation for battery powered propulsion systems is given in Equation 11 below.

$$t_{END} = \frac{Ahr_{BATT}}{Amps_{TOTAL}} = \frac{BatteryCapacity(AHr)}{CurrentDraw(Amps)} \quad (11)$$

Equation 11 takes the amount of amps the motor draws to produce enough thrust for flight and divides it into the energy content of the battery rated in Amp-hours. This gives the total hours of flight possible based on a known current draw.

EXPERIMENTAL SETUP

The Mechanical and Aerospace Engineering Department at the University of Dayton houses a low-speed wind tunnel (LSWT) for experimental use. The wind tunnel is of the Eiffel-type with a contraction ratio of 16:1, an overall length of 48.5 ft. and interchangeable test sections which are 30" by 30" by 96" in length. The inlet freestream turbulence intensity is less than 0.1 percent and the maximum velocity is 40 m/s. The test section that was used had a Unistrut mounting apparatus that was utilized to integrate the motors and instrumentation to the tunnel test section base. This was initially constructed to integrate properly with a 25 lb S-beam load cell as thrusts greater than 25 lbs were not expected. It was discovered however that the moment the torque sensor and motors placed on the S-beam load cell was beyond its recommended tension value, and a new 100 lb cantilever beam load cell was then used. This Omega brand LC 501 load cell had an accuracy of $\pm 0.041\%$ of full output, having each reading being accurate to ± 0.041 lbs. The torque sensor that was used was a Futek TFF350 with an output of ± 8.33 ft-lbs. The torque sensor had an accuracy of $\pm 0.3\%$ full output, possibly varying each reading by ± 0.025 ft-lbs. The system that was designed for the experiments can be seen in Figure 2.

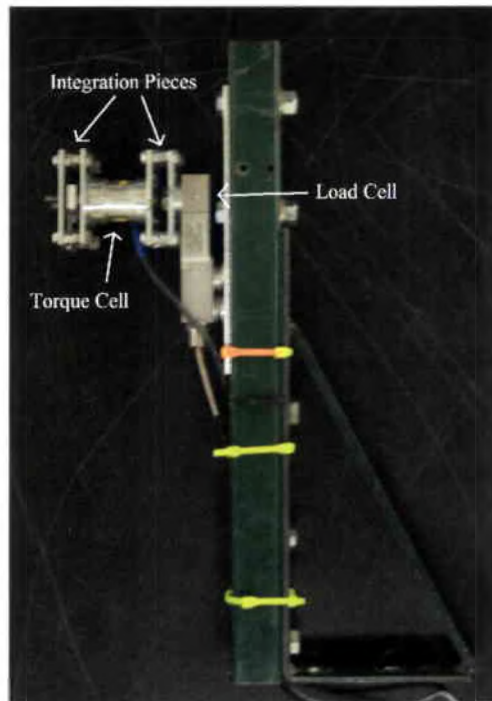


Figure 2 - Instrument Base Configuration

An interface, seen above, was necessary to connect the load cell to the torque cell which is also seen in the above figure. This was necessary in order to take simultaneous torque and thrust measurements. Figure 2 shows the basic instrumentation attached to the Unistrut that integrates to the base of the wind tunnel. The three Hacker motors that were evaluated were:

- Hacker B20-18L
- Hacker B40-10S
- Hacker B40-10L.

All were equipped with a manufacturer installed gear box with a 4:1 gear ratio. Figure 3 shows the Hacker motor integration point, to the instrumentation portion of the apparatus in Figure 2.

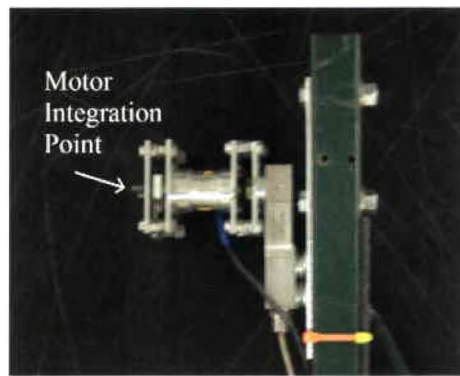


Figure 3 - Electric Motor Instrumentation Configuration (side view)

A universal interface was fabricated to connect each motor to the torque cell. This universal piece has the ability to integrate with all of the motors tested. The two bolts seen on the left side of the integration piece, where the arrow is pointing in Figure 3, is able to secure both motor mounts to the assembly. The two electric motor mounts were also fabricated to hold the motors while offering the least amount of surface area to reduce propeller backwash. One motor mount was for the B20 and one was for the two B40's. Two were required since the B40 motors would produce significantly more torque and thrust than the B20, so the B40 mount needed to be stronger. Figure 3 shows a top view of how the motors interfaced with their respective motor mount. The B40 motors integrated with the mount on the left and the B20-18L integrated as shown in the right mount.



Figure 4 - Motor Integration (top view)

The propellers were mounted where the shaft is seen coming out of the mount on the top side of Figure 4. The bottom side of the mount is where each motor mount interfaced with the integration piece that connected it to the torque cell and the rest of the instrumentation.

The mounts described above allowed the simultaneous measurement of torque, thrust, and RPM in order to perform the desired efficiency analysis. The RPM was measured using a strobe with variable frequency that was matched to the propeller's rotation frequency. Symbols were drawn on each blade of the propeller to ensure that the RPM recorded was the true RPM and not double the true RPM as both scenarios would have the propeller appear to have the correct strobe frequency.

Controlling the brushless DC motors required the use of an electronic speed controller (ESC). At first a Jeti Advanced 90 Plus ESC was used. This ESC only allowed hard and soft time modes based on the poles of the motor that it would be controlling. This corresponded to the rate at which the ESC would switch between the three phases it ran into the motor, causing it to spin. Hard timing would be for higher performance motors and soft timing would be for lower performance motors. Whether or not a motor is high performance or not is usually dictated by the number of poles a motor has, the larger the higher the performance. All of the Hacker motors were two pole motors so soft timing was set based on the instructions for the Jeti Advanced 90 Plus. It was determined that this was not enough of a timing specification as the motors overheated very easily when run above 70% throttle. After consulting Hacker themselves, it was recommended to use a Jeti SPIN 66 ESC. This came with a programming box that allowed the user to set the

exact degree of timing for the motor, allowing it to operate safely and not overheat as easily. All of the Hacker motors tested were set at 2 degrees. This programming box also allowed various other settings such as propeller spin direction, temperature cutoff, minimum timing point in milliseconds, maximum timing point in milliseconds, and controller frequency. The timing points corresponded to 0% and 100% throttle settings. Along with the new ESC it was recommended to power the motors at 10 V as opposed to the initial 15 Volts. This worked extremely well and solved the overheating issue.

Controlling the throttle in precise intervals was also not possible using conventional receivers and transmitters. A servo tester was purchased from a local hobby shop that connected to the three wire ESC input. The servo tester had a dial that could be toggled between the minimum 1.0 millisecond (ms) position for 0% throttle and the maximum setting of 2.0 ms for 100% throttle. This assured repeatability for accurate throttle settings. The servo tester can be seen in Figure 5.

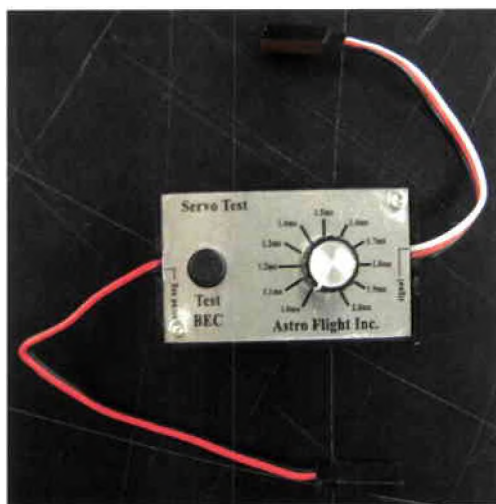


Figure 5 - Throttle Controlling Servo Tester

The ESC/motor system was powered by a regulated power supply that had a maximum output of 3.5 kW. The power cables were connected through a Medusa Research Inc Power Analyzer Pro box, seen in Figure 6, that connected to a PC through USB cables, allowing for accurate voltage and current data to be read. The Power Analyzer Pro had an accuracy of $\pm 0.1\%$ for both current and voltage readings. The Power Analyzer Pro also had the ability to control the throttle from the laptop but the timing was found to be inaccurate, and the motor would peak at 60% throttle. The servo tester shown in Figure 5 proved to be a more reliable and accurate way to control the throttle in the experiment.



Figure 6 - Medusa Research's Power Analyzer Pro

For each test run the atmospheric conditions were recorded and used to calculate the necessary manometer reading in inches of water to attain the desired wind tunnel speed. The parameters recorded were temperature, humidity, and pressure. The three wind tunnel speeds for each motor were determined from real world operating conditions in order to evaluate each system in an accurate scenario. The propellers were not intended to be a variable in the analysis of the motors, as a propeller study could have presented a whole new avenue of research. With that in mind, propellers were chosen in the middle of the recommended propeller size ranges. For example if the largest recommended propeller for a given motor was a 12x8 and the smallest was an 8x4, a 10x6 was used to

provide an average propeller. All motor and propeller combinations were executed at 60, 70, 80, and 90 percent throttle. Table 1 on the following page shows the different runs that were completed.

Table 1 - Motor Test Run Matrix

<u>Motor and Propeller</u>	<u>Set Wind Tunnel Speed</u>	<u>Throttle Variations</u>
B20-18L 10x7 SLOW	10 mph	60, 70, 80, 90 %
B20-18L 10x7 SLOW	20 mph	60, 70, 80, 90 %
B20-18L 10x7 SLOW	35 mph	60, 70, 80, 90 %
B40-10S APC-E 12x6	20 mph	60, 70, 80, 90 %
B40-10S APC-E 12x6	35 mph	60, 70, 80, 90 %
B40-10S APC-E 12x6	50 mph	60, 70, 80, 90 %
B40-10L APC-E 14x8.5	25 mph	60, 70, 80, 90 %
B40-10L APC-E 14x8.5	40 mph	60, 70, 80, 90 %
B40-10L APC-E 14x8.5	55 mph	60, 70, 80, 90 %

For each of the test run combinations listed above RPM, torque, induced velocity, and thrust were recorded. It was discovered that when the tests were performed and the motors powered up the velocity through the wind tunnel increased from the initially set wind tunnel speed. This was the induced velocity that was recorded using the manometer and the same induced velocity used in the calculations of power and efficiency since this was the new velocity the propeller motor combination would be experiencing. As described above the RPM was measured using a strobe light where the frequency was

increased until the blades of the propeller were standing still, and it was verified that it was not doubled by the fact the symbols drawn on each of the two blades were not overlapping. The torque and thrust were measured using a high precision multimeter which offered readings to the thousandths of millivolts (mV). These readings were recorded and then used to calculate the output of each instrument based on the calibrated output of the instrument with known loads. The load cell was calibrated to be 0.291 mV/lb and the torque cell to be 3.211 mV/ft-lb. The induced velocity needed to be noted since the propeller was able to speed up the air moving through the test section, allowing the disk plane of the propeller to experience a velocity higher than what the wind tunnel was set at. This was measured by recording the new manometer reading with the throttle up, and back calculating to a wind speed using the same method stated above for the initial speed setting of the wind tunnel. Figure 7 shows all of the instrumentation and equipment integrated together inside of the wind tunnel test section that was used. It should be noted here though that Figure 7 shows 6 of the 13 pressure taps that the wind tunnel test section had placed in it. They are nearly evenly spaced as seen, with their exact longitudinal locations in reference to the disk plane found in Table 23 of Appendix A. The Numbering convention was in reference to each motor's disk plane location. Zero was at the disk plane itself and positive numbers represented upstream locations and negative numbers were at downstream taps. The B20 mount was shorter due to the motor's shorter length, so its x-longitudinal test section position values would be larger upstream and less downstream than the B40 motors. Basically the fact the B20 is shorter and has a shorter motor mount, its disk plane is moved closer to the back allowing the farthest forward pressure tap to be at a greater distance away from the disk plane than the

same tap on the B40's. The use of these taps will be explained further in the following section.

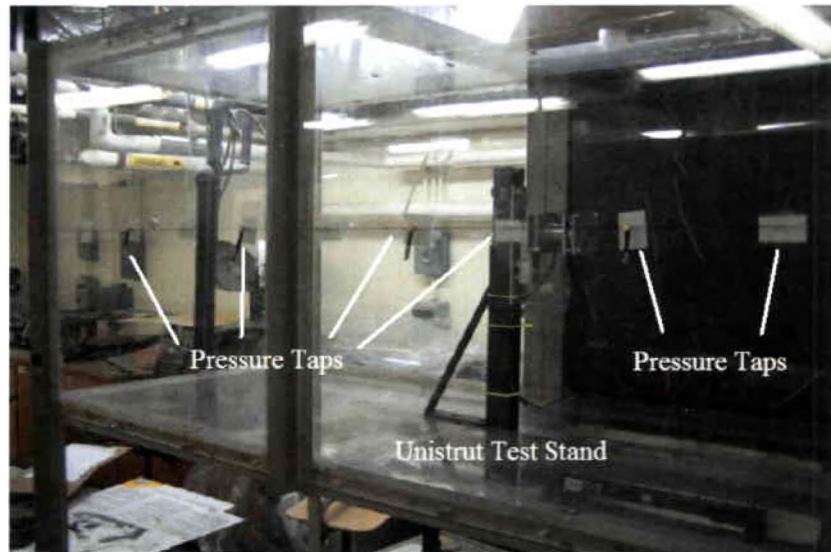


Figure 7 - Unistrut Test Stand mounted in Wind Tunnel

RESULTS

The entire test matrix was executed numerous times with only a small variance of the data, between 1 and 2%, varying between runs, demonstrating the repeatability of the data under the current setup. Tables 11-19 in Appendix A show the initial data that was taken with only Glauert's velocity correction applied to the induced velocity. Glauert's correction is shown in the tables as 'Ind Velocity Glauert'.

B20-18L

For the B20 case, the efficiency numbers look reasonable for the two slowest runs of 10 and 20 mph, which can be seen in Appendix A in Tables 12 and 13 respectively. The 35 mph run seen in Table 14 in Appendix A, did not appear to be as well understood as it had impossibly high efficiencies for both the propeller and propulsive efficiency. This is thought to be due to the blockage effect of the propeller on the freestream air in a smaller than needed wind tunnel cross section. The efficiency numbers in the table were calculated using Glauert's velocity correction and shows that it is not enough of a correction for this as well as the other two motors. It is suspected that the middle 20 mph case also has a degree of wall interference but it is not as obvious as the 35 mph case. It makes sense that this would not occur until higher wind tunnel speeds, as this is the case when there is a greater mass flow rate of air moving through the tunnel. If there is not sufficient space for the air to flow around the disk plane then it will create a blockage

effect and will distort the data. A method that corrects the data more appropriately than Glauert's correction will be discussed in detail in the Additional Correction Methods section.

B40-10S

The B40-10S motor showed reasonable data at the lowest speed of 20 mph which can be found in Table 15 in Appendix A, but showed wall interference effects in both the 35 mph and 50 mph cases seen in Appendix A in Tables 16 and 17 respectively. This is subtle when looking at the 60% throttle case in Table 16. The reported propeller efficiency was 90.9% which is theoretically not impossible but most real world propeller efficiencies at higher Reynolds Numbers occur between 65% and 85% giving the hint of wall interference. Wall effects are very obvious when looking at Table 17 and the 50 mph case since the propeller efficiency is over 100% again. The propeller for the B40-10S is larger than that of the B20-18L so it is expected that the effects of the blockage will be more obvious at lower wind tunnel speeds. For this reason all of the runs of the B40-10S are expected to have a degree of blockage due to wall interference and will be examined in the next section.

B40-10L

The B40-10L was by far the most obvious motor that needed to be corrected due to freestream blockage. It comes as no surprise since it not only utilized the largest propeller but also ran at higher speeds than the other two motors. Its slowest test run of 25 mph seen in Table 18 of Appendix A, attained a propeller efficiency of 84.8% which

again is not impossible; it is just at the high end of real world expected values for propeller efficiency. Tables 19 and 20 located in Appendix A, which show test runs at 40 and 55 mph respectively, definitely need to be corrected by a means other than Glauert as they both have propeller efficiencies greater than 100%. Again, this will be examined in detail in the next section.

Additional Correction Methods

As can be seen in the previous section, the Glauert correction for velocity was not enough to give reasonable efficiency numbers at high wind tunnel speeds and propeller diameters. As a comparison, B20-18L had a propeller with a diameter of 10 inches. This corresponds to a circular area of 0.55 ft^2 . The wind tunnel has a cross sectional area of 6.25 ft^2 giving a blockage ratio of 8.8%. The B40-10S had a 12 inch propeller which corresponded to a blockage ratio of 12.5%, and for the B40-10L a ratio of 17.1% with its 14 inch propeller. These cases are too large for the Glauert correction, seen in Equation 4, to accurately produce meaningful data. The main method that was used to correct the data was one described in the Hackett, Wilsden, and Lilley paper that used wall static pressure readings. The Hackett method that was described in great detail in their paper, utilized the superposition of a uniform freestream over a point source to develop their correction method. When looking at flow in a wind tunnel test section, the freestream flow is not able to freely move around objects in the tunnel causing the flow to be effected both upstream and downstream. The problem came in how to correctly model

the entire situation and develop a correction. Figure 8 illustrates the idea of a point source in a confined flow situation with a superimposed uniform freestream.

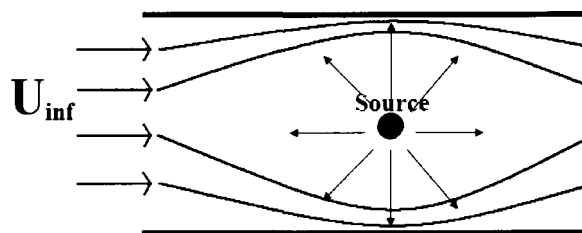


Figure 8 - Point Source Theory in Wind Tunnel

As freestream flow enters the test section of the wind tunnel that has a point source in it, the flow is diverted around the source, causing the stream lines to converge thereby accelerating the flow. By taking wall pressure measurements along the span of the tunnel test section, the behavior of the flow can be readily modeled. The strength of the source would then be determined by the pressure measurements along the wall which would lead to the buoyancy correction for the thrust of the motor. The Hackett method had both asymmetric and symmetric analysis involved in the original correction procedure for use with lifting bodies. For this experiment that utilized a symmetric disk plane, the correction method was assumed to be entirely symmetric.

For this effort, thirteen wall static pressure measurements were taken along the length of the test section using pressure taps that screwed into the side of the wind tunnel. The thread size was a standard #10-32 and had a ribbed pressure port that was easily attached to the manometer for recording the pressure data. A close up of one of the pressure ports can be seen in Figure 9.

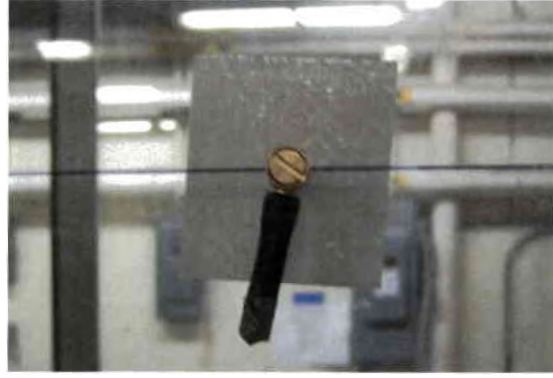


Figure 9 - Pressure Tap Close Up

The manometer provided readings with an accuracy of ± 0.002 inches of water or $\pm 7.23 \times 10^{-5}$ pounds per square inch (psi). These readings were taken at all thirteen ports, for all motors, at all power settings. When a port was not being read from a sealed black hose was placed over its opening as seen in Figure 9. When readings were taken, the black sealed hose was removed and the manometer tubing was placed over the tap opening. Readings with the tunnel completely empty were also necessary at all wind tunnel speeds as a reference baseline for the powered pressure readings described above. Equation 12 was used to convert the pressure measurements, modified into coefficients of pressure, into velocity changes normalized by the free stream velocity.

$$\frac{\Delta u}{U_{\infty}} = \sqrt{1 - (C_{P_{EMPTY}} - C_{P_{POWERED}})} - 1 \quad (12)$$

These $\frac{\Delta u}{U_{\infty}}$ values were then plotted at their x streamwise longitudinal position normalized by the total length of the test section b , for a final x-axis variable of x/b . These plots can be seen below starting with the lowest speed which was expected to be the least accurate due to the significantly large changes in pressure from point to point

downstream of the disk plane. The trend is what was being used in the correction and not the actual data due to the low signal to noise ratio.

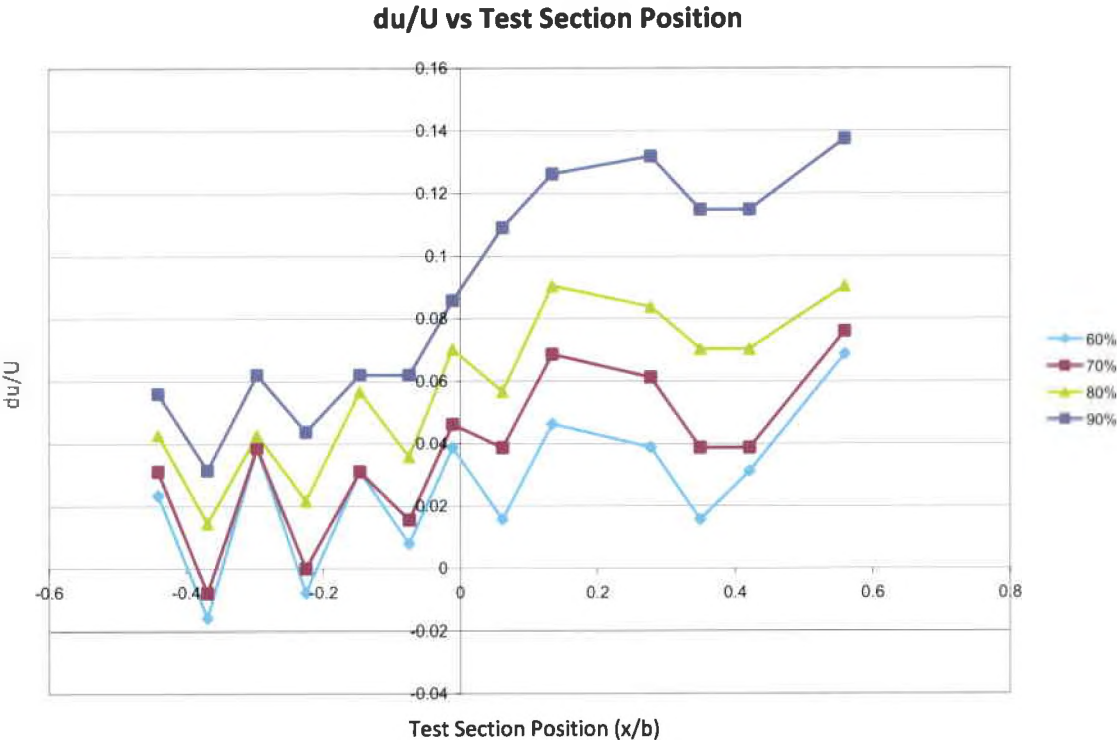


Figure 10 - B20-18L Velocity Profile at 10 mph

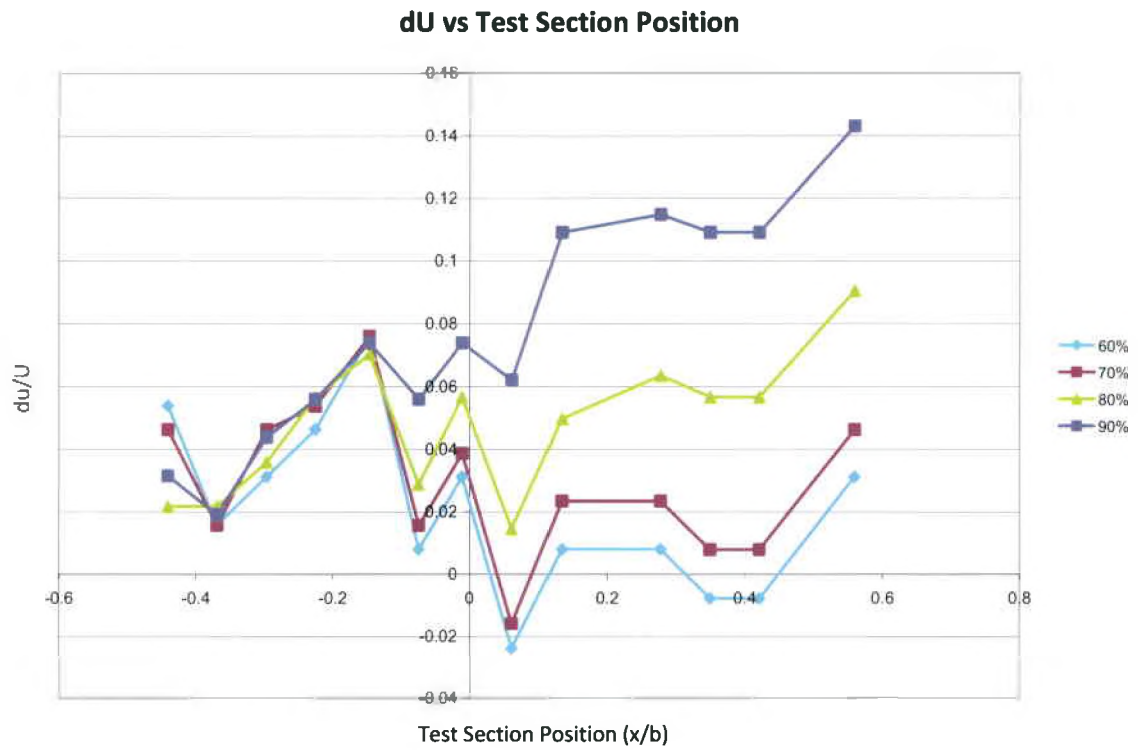


Figure 11 - B20-18L Velocity Profile at 20 mph

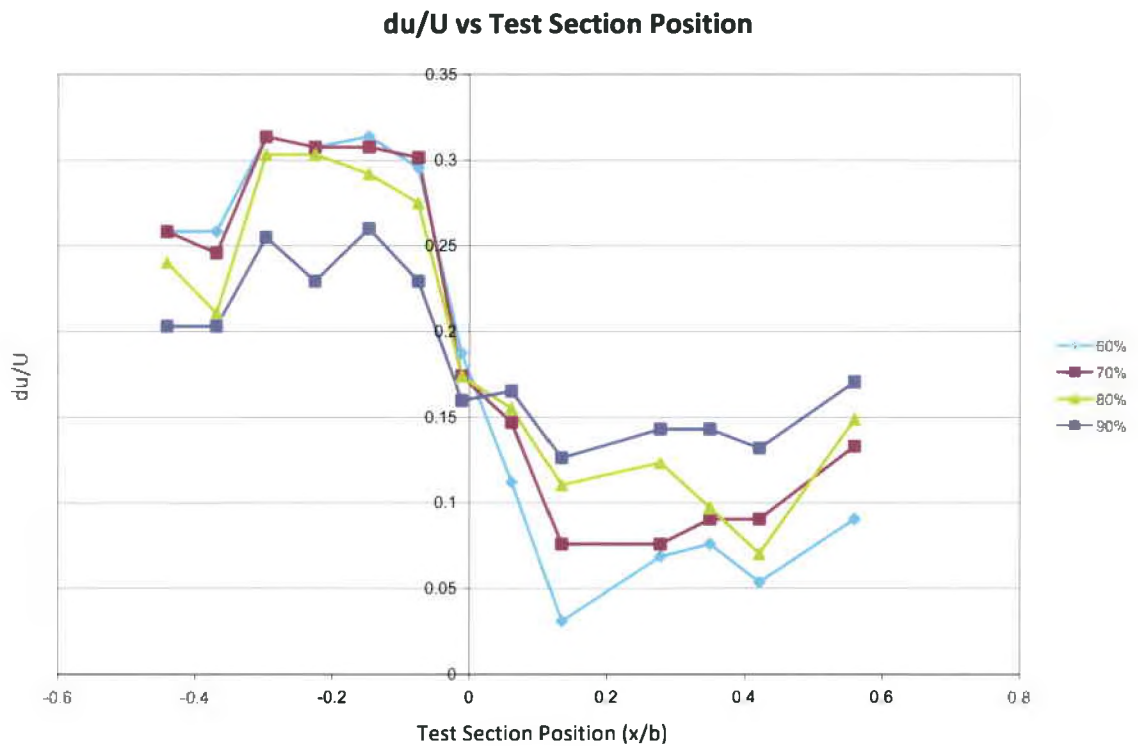


Figure 12 - B20-18L Velocity Profile at 35 mph

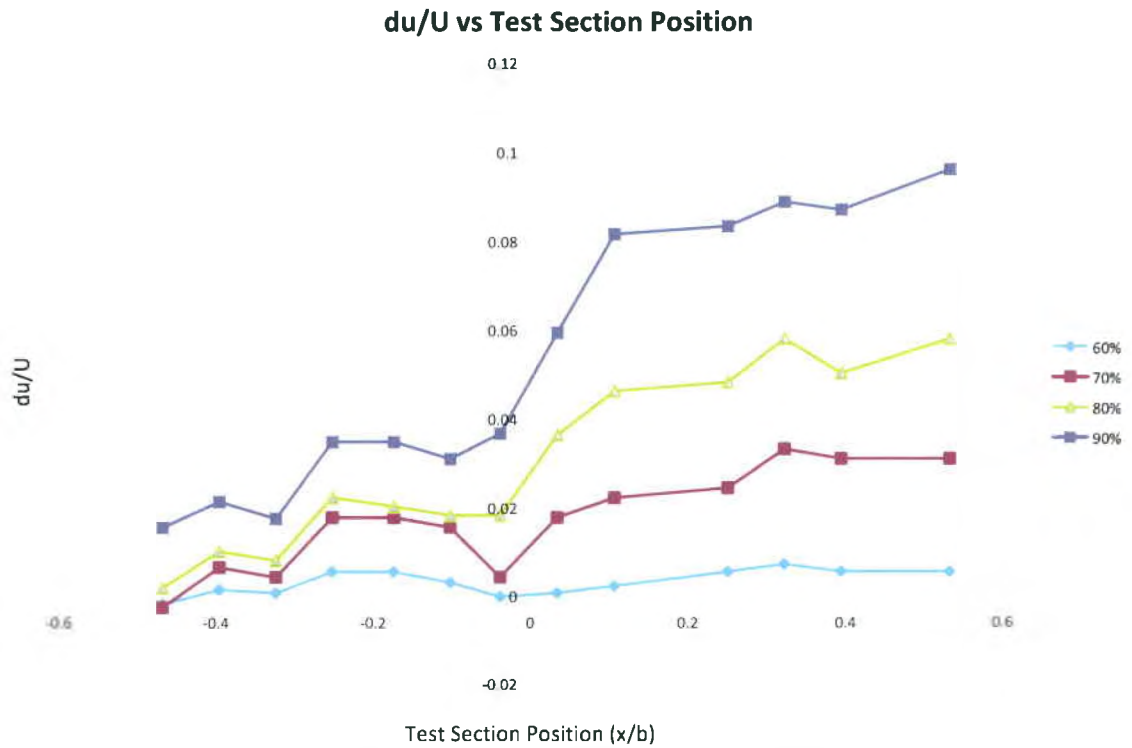


Figure 13 - B40-10S Velocity Profile at 20 mph

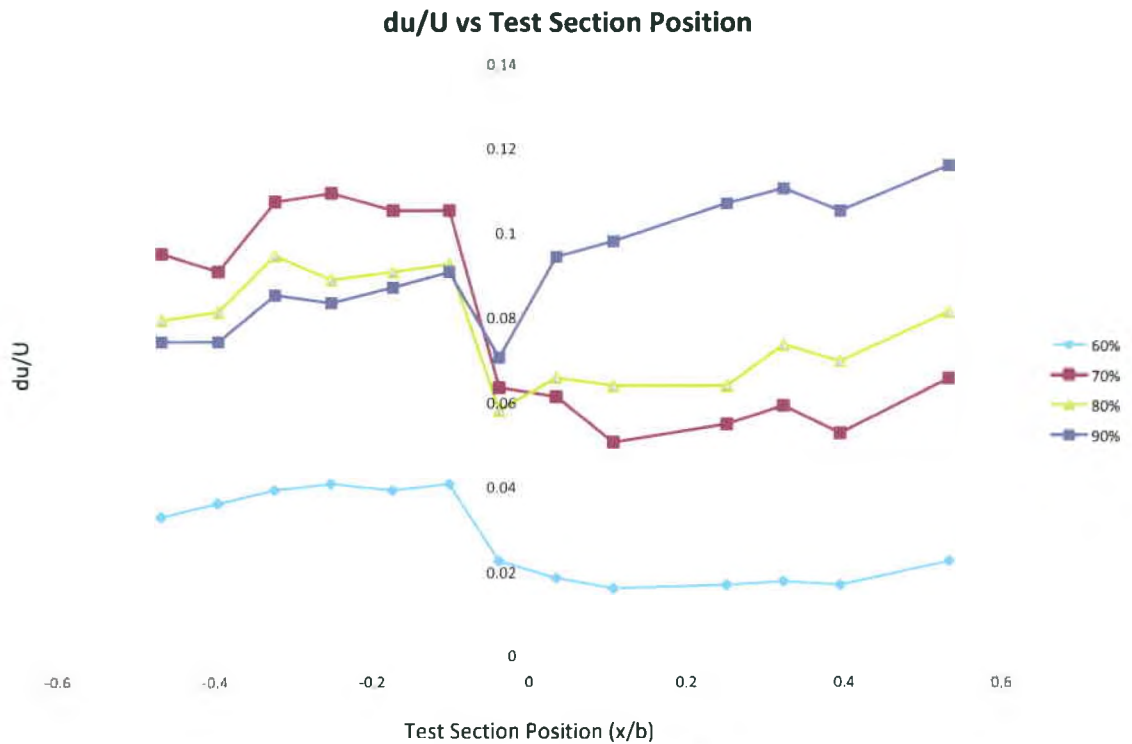


Figure 14 - B40-10S Velocity Profile at 35 mph

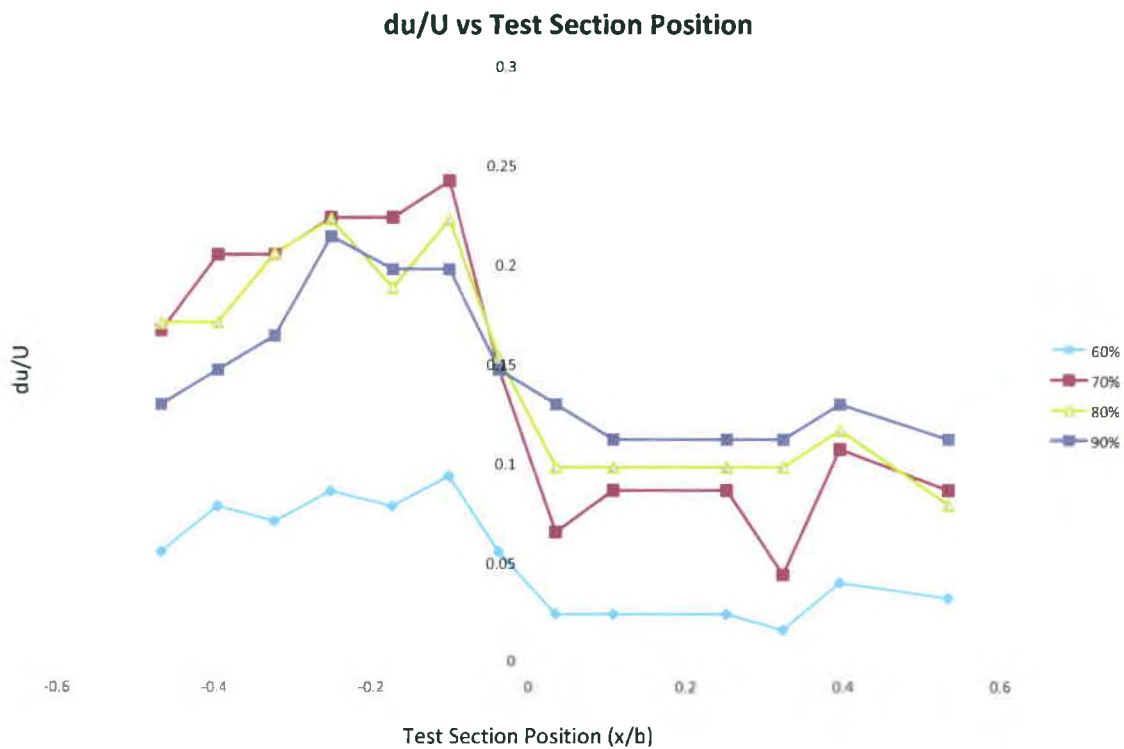


Figure 15 - B40-10S Velocity Profile at 50 mph

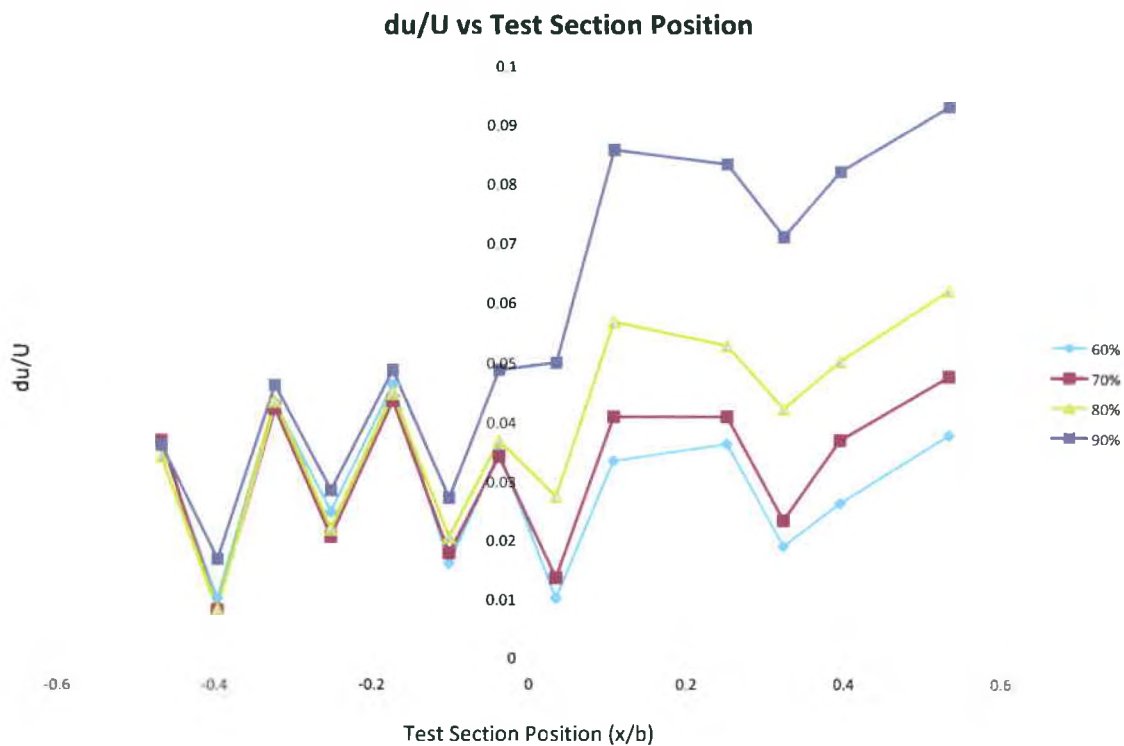


Figure 16 - B40-10L Velocity Profile at 25 mph

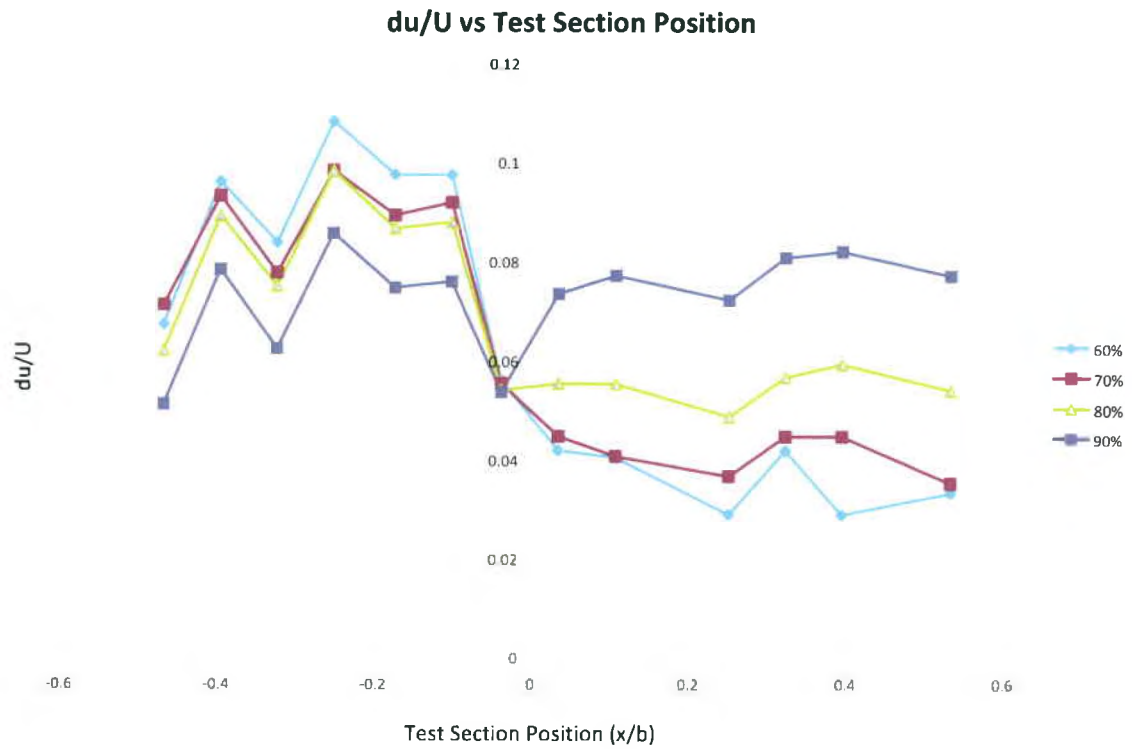


Figure 17 - B40-10L Velocity Profile at 40 mph

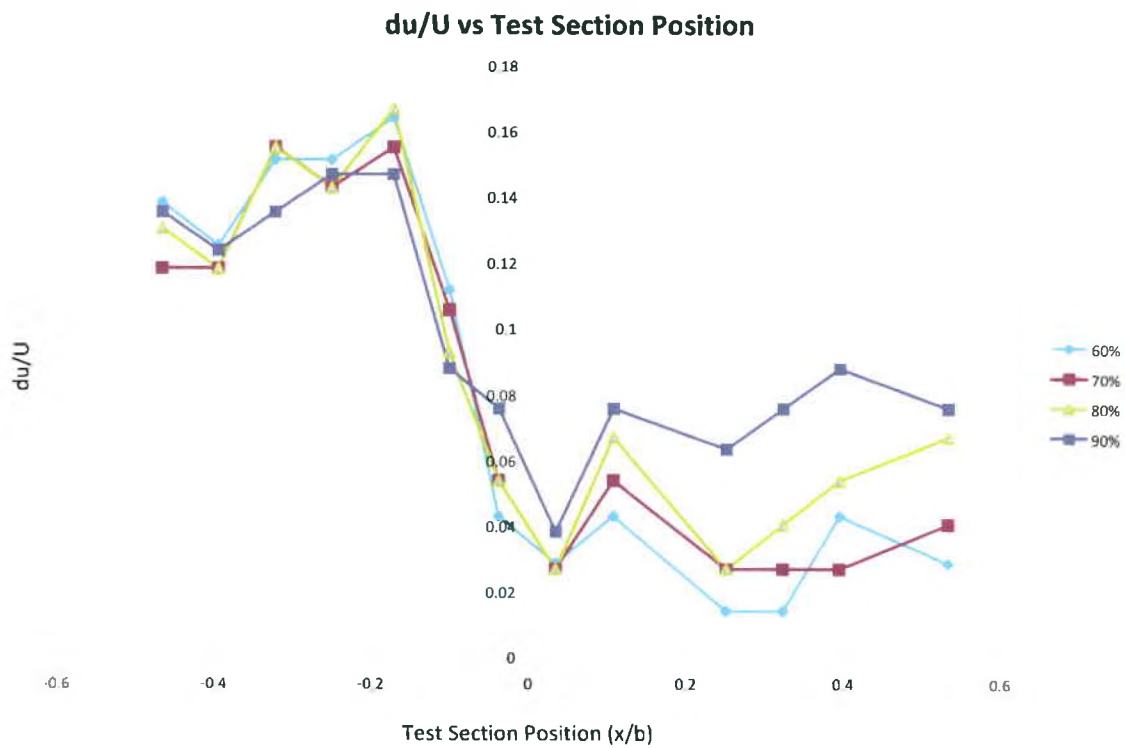


Figure 18 - B40-10L Velocity Profile at 55 mph

The method in that was developed by Hackett, Wilsden, and Lilley requires the far downstream value of $\frac{\Delta u}{U_\infty}$ that theoretically should form a horizontal asymptote. This is illustrated in Figure 19.

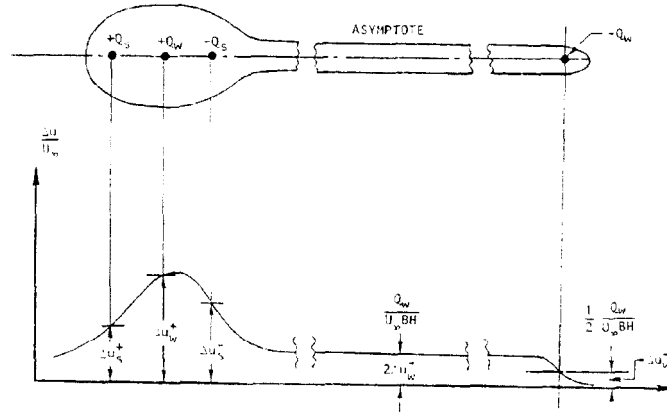


Figure 19 - Hackett, Wilsden, and Lilley's Asymptote Description

This plot in Figure 19 came directly from the Hackett, Wilsden, and Lilley paper referenced in the Literature Search section. Their axis convention was different than the one used here as their far downstream parts of the graph are all positive x-axis values and not negative. It can be seen that in an ideal setup configuration, enough downstream test section span is available to allow the $\frac{\Delta u}{U_\infty}$ values to settle to an asymptotic value. For the plots in Figures 10-18 this asymptotic value was at the far negative end of the x-axis. Although a clear asymptote was not visible in the plots an educated inference was made in order to calculate the correction. From these plots the downstream asymptotic $\frac{\Delta u}{U_\infty}$ value of each power curve at each velocity was noted and substituted into Equation 13 to yield the value of A_5 .

$$A_5 = 0.5 \cdot \left(\frac{\Delta u}{U_\infty} \right)_{MIN} \quad (13)$$

Where $\left(\frac{\Delta u}{U_\infty} \right)_{MIN}$ is the downstream asymptotic value of each power curve, 60%-90%, at each wind tunnel speed and for each motor. The result of Equation 13 was then is substituted into Equation 14 to yield the wake blockage source strength Q_w .

$$Q_w = 2 \cdot A_5 \cdot C \cdot U_\infty \quad (14)$$

Where C is the tunnel cross sectional area of 6.25 ft^2 , and U_∞ is the tunnel free stream velocity. Q_w is then input into Equation 15 to yield the change in drag force that is necessary to correct the data.

$$\Delta Drag = 0.5 \cdot \rho \cdot \frac{Q_w^2}{C} \quad (15)$$

The table for the variables found in Equations 13-15 can be seen in Tables 21-23 in Appendix A.

The Delta Drag values for each motor, wind tunnel speed, and power setting were then subtracted from the thrust values of the respective test run data set and represent Thrust Corrected in the tables that follow. This thrust corrected then went into the calculations of THP, Propeller Efficiency, and Propulsive Efficiency in the Hackett column in the following tables. The same Glauert values were calculated using the Induced Velocity Glauert value from the previous tables. This is why the Glauert method velocities are different from the other two columns. Along with the corrected data, the same tables have the original measured test data that is uncorrected.

When analyzing the symmetric correction developed by Hackett there were a number of variables other than A_5 and Q_w that were calculated and used in the analysis. Since this experiment only required horizontal buoyancy correction, the delta drag equation was all that was focused on. Looking at Equation 15 it can be seen that it only varies with C , A_5 , and Q_w . Hence eliminating the need to determine the other variables.

B20-18L

Table 2 - B20-18L Corrected Data at 10 mph

60%				
<u>Metric</u>	<u>Uncorrected</u>	<u>Glauert</u>	<u>Hackett</u>	<u>Theoretical</u>
Ind Velocity (mph)	11.36	11.04	11.36	11.36
Thrust (lb)	0.409	0.409	0.409	0.3918
Torque (lb-ft)	0.0343	0.0343	0.0343	0.0283
THP (hp)	0.0124	0.0121	0.0124	0.0119
BHP (hp)	0.0218	0.0218	0.0218	0.0180
Propeller Eff	0.568	0.552	0.568	0.658
Propulsive Eff	0.311	0.302	0.311	0.298
70%				
<u>Metric</u>	<u>Uncorrected</u>	<u>Glauert</u>	<u>Hackett</u>	<u>Theoretical</u>
Ind Velocity (mph)	11.36	10.95	11.36	11.36
Thrust (lb)	0.602	0.602	0.601	0.5461
Torque (lb-ft)	0.0489	0.0489	0.0489	0.0375
THP (hp)	0.0182	0.0176	0.0182	0.0165
BHP (hp)	0.0357	0.0357	0.0357	0.0273
Propeller Eff	0.512	0.493	0.511	0.605
Propulsive Eff	0.307	0.296	0.307	0.279
80%				
<u>Metric</u>	<u>Uncorrected</u>	<u>Glauert</u>	<u>Hackett</u>	<u>Theoretical</u>
Ind Velocity (mph)	11.83	11.31	11.83	11.83
Thrust (lb)	0.915	0.915	0.913	0.7889
Torque (lb-ft)	0.0735	0.0735	0.0735	0.0521
THP (hp)	0.0289	0.0276	0.0288	0.0249
BHP (hp)	0.0631	0.0631	0.0631	0.0447
Propeller Eff	0.458	0.438	0.457	0.557
Propulsive Eff	0.292	0.279	0.292	0.252
90%				
<u>Metric</u>	<u>Uncorrected</u>	<u>Glauert</u>	<u>Hackett</u>	<u>Theoretical</u>
Ind Velocity (mph)	12.62	11.92	12.62	12.62
Thrust (lb)	1.586	1.586	1.581	1.3311
Torque (lb-ft)	0.1267	0.1267	0.1267	0.0838
THP (hp)	0.0534	0.0504	0.0532	0.0448
BHP (hp)	0.1382	0.1382	0.1382	0.0914
Propeller Eff	0.386	0.365	0.385	0.490
Propulsive Eff	0.252	0.238	0.251	0.212

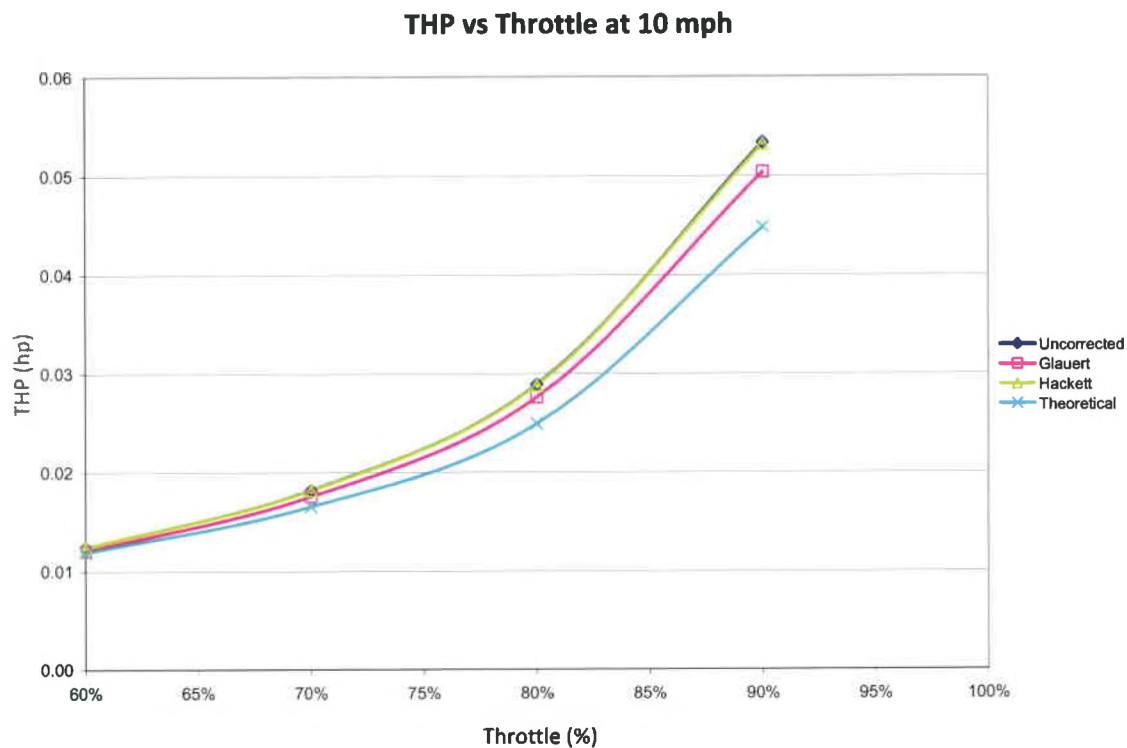


Figure 20 - B20-18L at 10 mph Correction Comparison

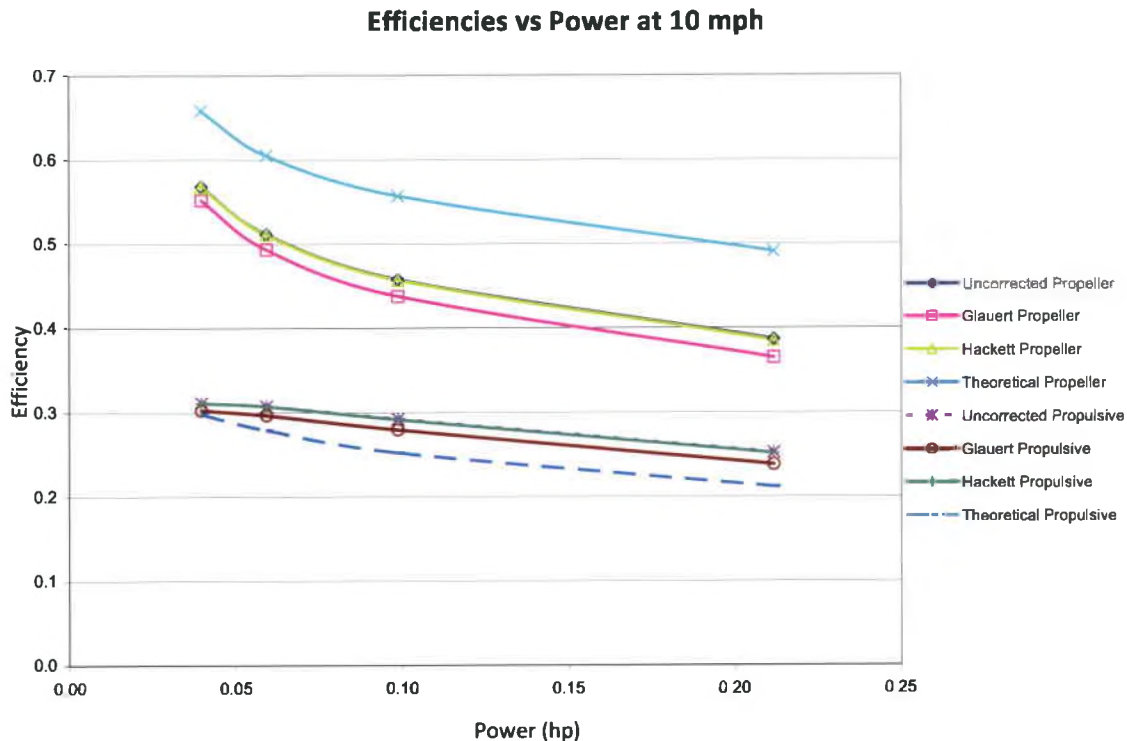


Figure 21 - B20-18L Efficiency Comparison at 10 mph

As expected of a small propeller at a low wind tunnel speed, the correction to the measured B20-18L was nominal using the Hackett correction but slightly more with the Glauert method. A Theoretical curve can be seen as well for comparative purposes. These theoretical data points came from a momentum-disk theory program developed by the Air Force Research Laboratory's Air Vehicles Directorate. The inputs to the program were propeller geometry, altitude, wind speed, and RPM. The data recorded in the wind tunnel runs were input into the program to calculate the data points seen in the theoretical curves.

Table 3 - B20-18L Corrected Data at 20 mph

<u>60%</u>				
<u>Metric</u>	<u>Uncorrected</u>	<u>Glauert</u>	<u>Hackett</u>	<u>Theoretical</u>
Ind Velocity (mph)	20.48	20.26	20.48	20.48
Thrust (lb)	0.347	0.347	0.341	0.2184
Torque (lb-ft)	0.0321	0.0321	0.0321	0.0217
THP (hp)	0.0190	0.0188	0.0186	0.0119
BHP (hp)	0.0217	0.0217	0.0217	0.0147
Propeller Eff	0.876	0.866	0.860	0.813
Propulsive Eff	0.498	0.493	0.489	0.313
<u>70%</u>				
<u>Metric</u>	<u>Uncorrected</u>	<u>Glauert</u>	<u>Hackett</u>	<u>Theoretical</u>
Ind Velocity (mph)	20.74	20.45	20.74	20.74
Thrust (lb)	0.499	0.499	0.493	0.3691
Torque (lb-ft)	0.0448	0.0448	0.0448	0.0333
THP (hp)	0.0276	0.0272	0.0273	0.0204
BHP (hp)	0.0344	0.0344	0.0344	0.0255
Propeller Eff	0.803	0.792	0.794	0.800
Propulsive Eff	0.478	0.471	0.473	0.354
<u>80%</u>				
<u>Metric</u>	<u>Uncorrected</u>	<u>Glauert</u>	<u>Hackett</u>	<u>Theoretical</u>
Ind Velocity (mph)	21.00	20.61	21.00	21.00
Thrust (lb)	0.774	0.774	0.771	0.6274
Torque (lb-ft)	0.0688	0.0688	0.0688	0.0515
THP (hp)	0.0433	0.0425	0.0432	0.0351
BHP (hp)	0.0618	0.0618	0.0618	0.0462
Propeller Eff	0.701	0.688	0.699	0.760
Propulsive Eff	0.450	0.442	0.449	0.365
<u>90%</u>				
<u>Metric</u>	<u>Uncorrected</u>	<u>Glauert</u>	<u>Hackett</u>	<u>Theoretical</u>
Ind Velocity (mph)	21.46	20.86	21.46	21.46
Thrust (lb)	1.455	1.455	1.451	1.1007
Torque (lb-ft)	0.1317	0.1317	0.1317	0.0825
THP (hp)	0.0833	0.0809	0.0831	0.0630
BHP (hp)	0.1447	0.1447	0.1447	0.0906
Propeller Eff	0.576	0.559	0.574	0.695
Propulsive Eff	0.408	0.396	0.407	0.308

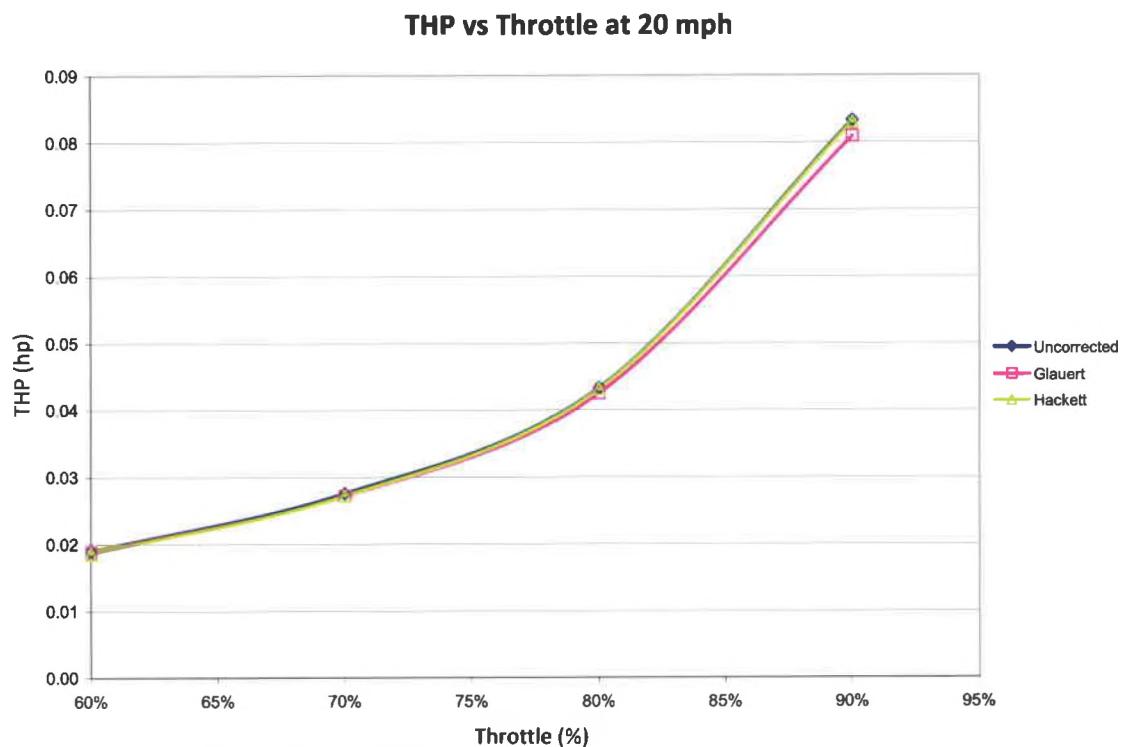


Figure 22 - B20-18L Thrust Horsepower Comparison at 20 mph

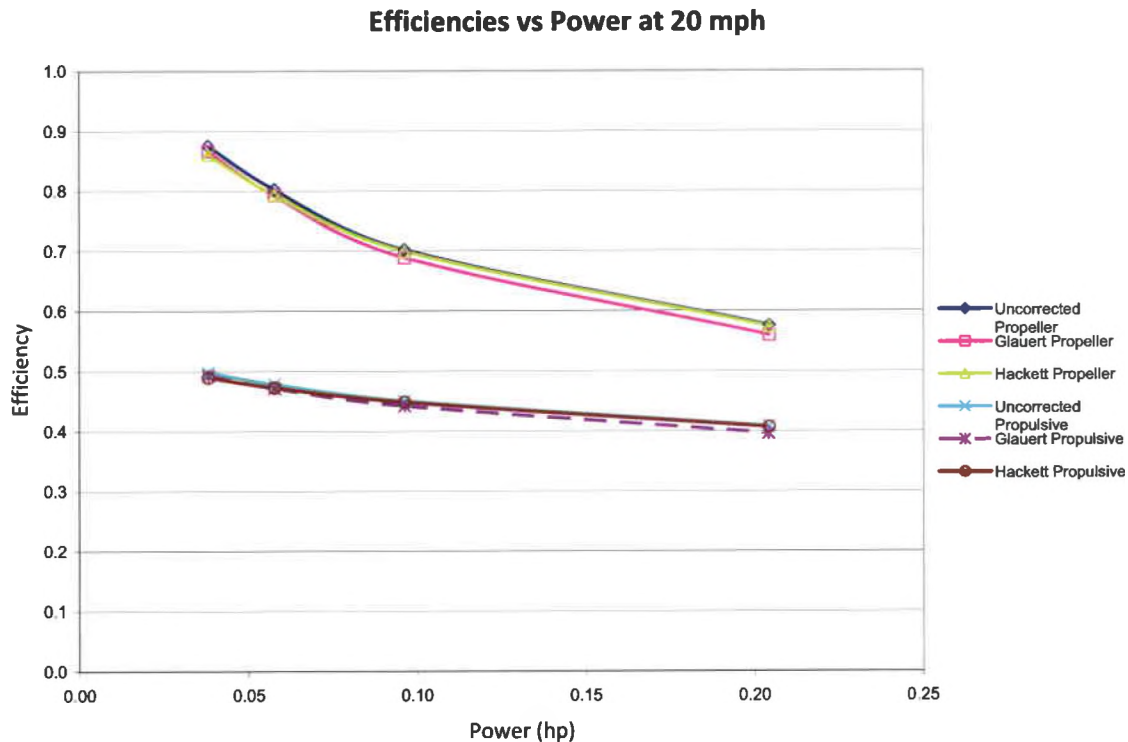


Figure 23 - B20-18L Efficiency Comparison at 20 mph

As with the 10 mph case, the B20-18L at 20 mph also required little change. The small propeller and relatively small wind tunnel speed did not create enough blockage to effect the data based on both the Glauert velocity correction and the Hackett thrust correction. The theoretical data curves are not plotted here because they differed from the measured data by a considerable amount.

Table 4 - B20-18L Corrected Data at 35 mph

<u>60%</u>				
<u>Metric</u>	<u>Uncorrected</u>	<u>Glauert</u>	<u>Hackett</u>	<u>Theoretical</u>
Ind Velocity (mph)	35.33	35.22	35.33	35.33
Thrust (lb)	0.268	0.268	-0.880	0.268
Torque (lb-ft)	0.0243	0.0243	0.0243	-0.1968
THP (hp)	0.0253	0.0252	-0.0829	-0.0142
BHP (hp)	0.0198	0.0198	0.0198	-0.0185
Propeller Eff	1.277	1.273	-4.190	-0.0116
Propulsive Eff	0.836	0.833	-2.742	1.602
<u>70%</u>				
<u>Metric</u>	<u>Uncorrected</u>	<u>Glauert</u>	<u>Hackett</u>	<u>Theoretical</u>
Ind Velocity (mph)	35.35	20.45	35.35	35.35
Thrust (lb)	0.372	0.499	-0.685	0.372
Torque (lb-ft)	0.0352	0.0448	0.0352	-0.0888
THP (hp)	0.0350	0.0272	-0.0645	-0.002
BHP (hp)	0.0306	0.0344	0.0306	-0.0084
Propeller Eff	1.146	0.792	-2.113	-0.0017
Propulsive Eff	0.753	0.471	-1.387	4.821
<u>80%</u>				
<u>Metric</u>	<u>Uncorrected</u>	<u>Glauert</u>	<u>Hackett</u>	<u>Theoretical</u>
Ind Velocity (mph)	35.76	35.53	35.76	35.76
Thrust (lb)	0.585	0.585	-0.316	0.585
Torque (lb-ft)	0.0564	0.0564	0.0564	0.1071
THP (hp)	0.0558	0.0554	-0.0302	0.018
BHP (hp)	0.0545	0.0545	0.0545	0.0102
Propeller Eff	1.024	1.017	-0.554	0.0174
Propulsive Eff	0.686	0.682	35.76	0.587
<u>90%</u>				
<u>Metric</u>	<u>Uncorrected</u>	<u>Glauert</u>	<u>Hackett</u>	<u>Theoretical</u>
Ind Velocity (mph)	35.63	35.23	35.63	35.63
Thrust (lb)	1.115	1.115	0.303	1.115
Torque (lb-ft)	0.1077	0.1077	0.1077	0.5939
THP (hp)	0.1059	0.1047	0.0288	0.0604
BHP (hp)	0.1241	0.1241	0.1241	0.0564
Propeller Eff	0.853	0.844	0.232	0.0696
Propulsive Eff	0.609	0.602	35.63	0.811

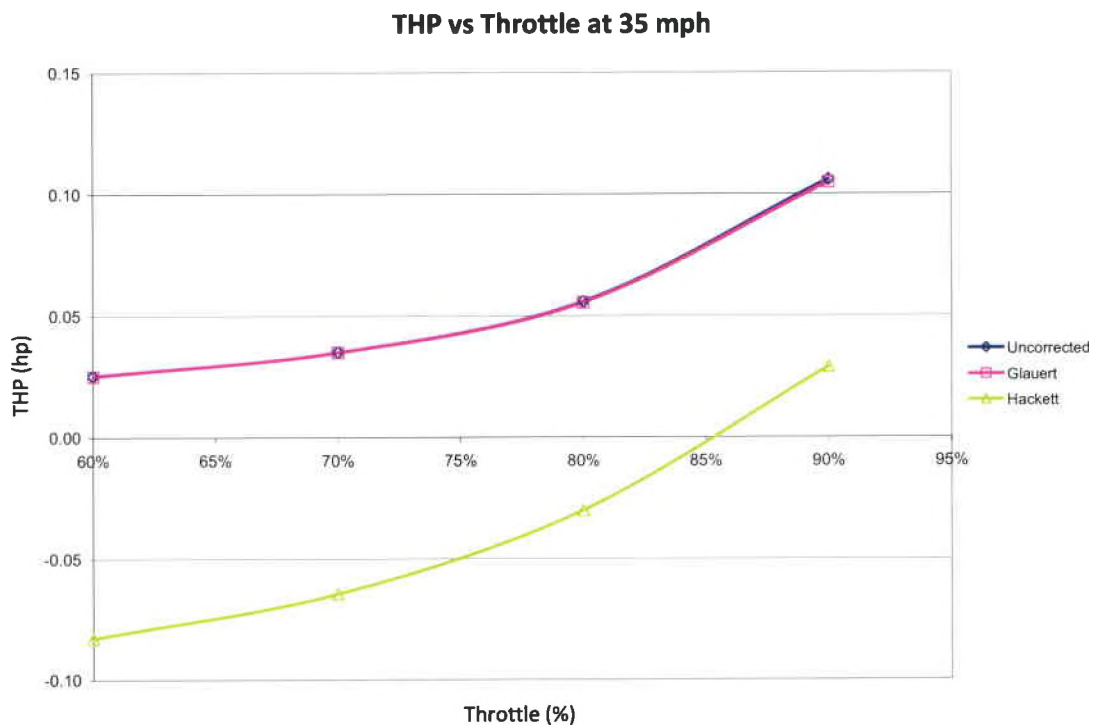


Figure 24 - B20-18L Thrust Horsepower Comparison at 35 mph

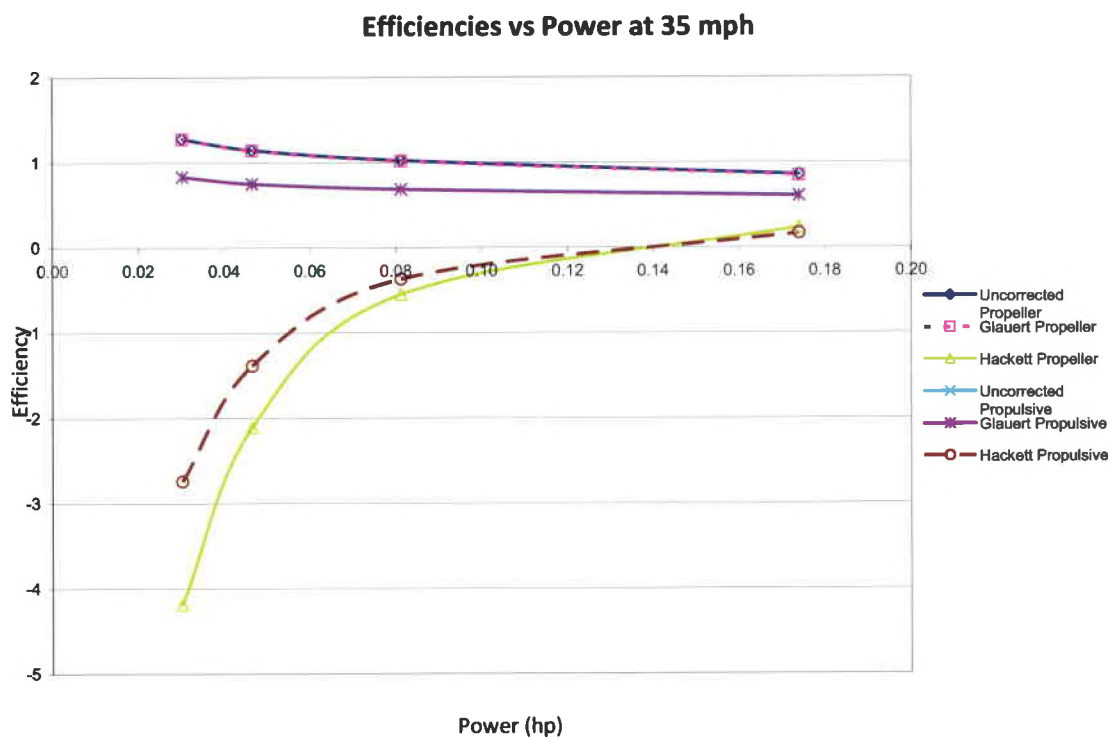


Figure 25 - B20-18L Efficiency Comparison at 35 mph

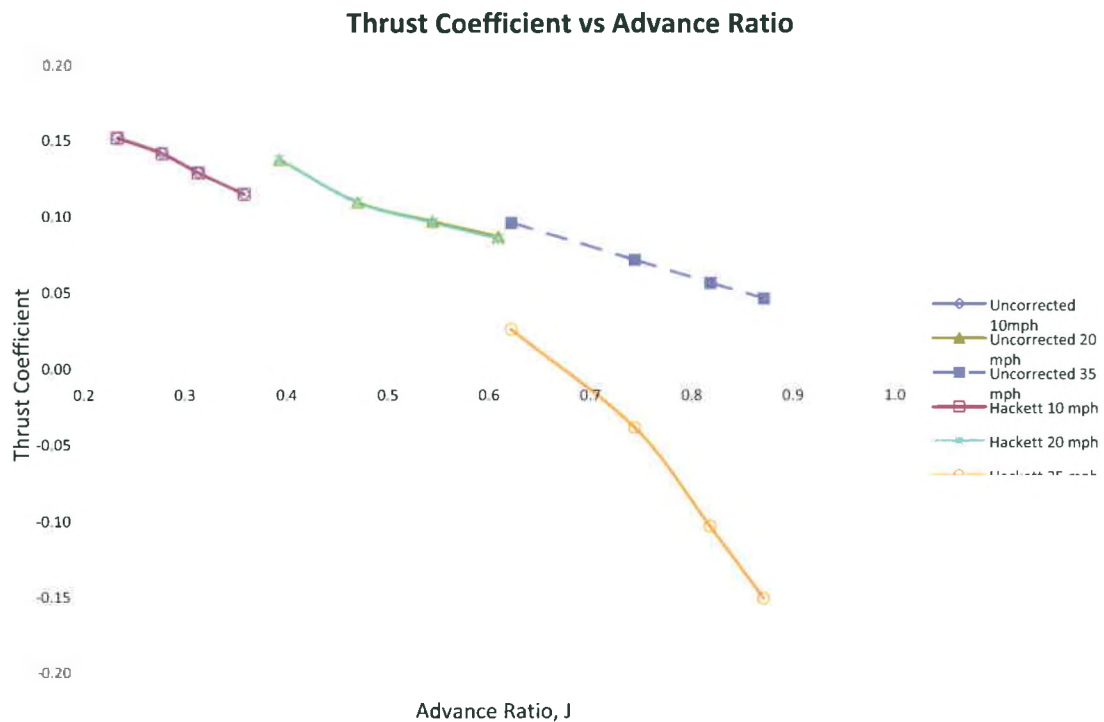


Figure 26 - B20-18L Thrust Coefficient vs Advance Ratio Plot

The 35 mph case for the B20-18L showed more relative correction which was expected based on the impossibly high measured propeller efficiency seen in Table 4. Glauert's velocity correction only corrected the data within a fraction of a percent while Hackett's thrust correction method based on wall static pressure measurements proved to be more applicable. The negative Thrust that can be seen in Table 4, and the negative values for THP, Propeller Efficiency, and Propulsive Efficiency seen in Table 4, as well as Figures 24 and 25 do make sense. At the lower power settings the propeller was not able to create enough thrust to overcome the drag force that the propeller disk plane enacted on the system. It was not until the motor was receiving 0.17 hp that the motor/propeller combination was able to produce positive thrust, but even then the THP it was producing

was minimal compared to the power going into the motor, producing a low propulsive efficiency.

Figure 26 shows a dimensionless comparison between the thrust coefficient and the advance ratio. The uncorrected data closely matches that of the data corrected using the Hackett method up until an Advance Ratio of just over 0.6. At this wind tunnel speed the propeller can no longer produce positive thrust and the thrust coefficient becomes negative. For this particular propeller geometry, that operating speed was much too high for the propeller to remain efficient at all. No theoretical results are represented because they also differed by a large margin.

B40-10S

Table 5 - B40-10S Corrected Data at 20 mph

60%				
Metric	Uncorrected	Glauert	Hackett	Theoretical
Ind Velocity (mph)	20.70	20.23	20.70	20.70
Thrust (lb)	0.843	0.843	0.843	0.849
Torque (lb-ft)	0.0747	0.0747	0.0747	0.0687
THP (hp)	0.0465	0.0455	0.0465	0.0469
BHP (hp)	0.0707	0.0707	0.0707	0.0650
Propeller Eff	0.658	0.643	0.658	0.721
Propulsive Eff	0.404	0.395	0.404	0.407
70%				
Metric	Uncorrected	Glauert	Hackett	Theoretical
Ind Velocity (mph)	21.21	20.63	21.21	21.21
Thrust (lb)	1.125	1.125	1.125	1.1028
Torque (lb-ft)	0.1018	0.1018	0.1018	0.0857
THP (hp)	0.0636	0.0619	0.0636	0.0624
BHP (hp)	0.1053	0.1053	0.1053	0.0887
Propeller Eff	0.604	0.588	0.604	0.704
Propulsive Eff	0.392	0.382	0.392	0.385
80%				
Metric	Uncorrected	Glauert	Hackett	Theoretical
Ind Velocity (mph)	22.19	21.31	22.19	22.19
Thrust (lb)	2.136	2.136	2.136	1.8814
Torque (lb-ft)	0.1647	0.1647	0.1647	0.1352
THP (hp)	0.1264	0.1214	0.1264	0.1113
BHP (hp)	0.2071	0.2071	0.2071	0.1699
Propeller Eff	0.611	0.586	0.610	0.655
Propulsive Eff	0.412	0.395	0.412	0.363
90%				
Metric	Uncorrected	Glauert	Hackett	Theoretical
Ind Velocity (mph)	22.67	21.52	22.67	22.67
Thrust (lb)	3.317	3.317	3.314	2.8953
Torque (lb-ft)	0.2435	0.2435	0.2435	0.1957
THP (hp)	0.2005	0.1903	0.2003	0.1750
BHP (hp)	0.3617	0.3617	0.3617	0.2907
Propeller Eff	0.554	0.526	0.554	0.602
Propulsive Eff	0.405	0.384	0.405	0.354

THP vs Throttle at 20 mph

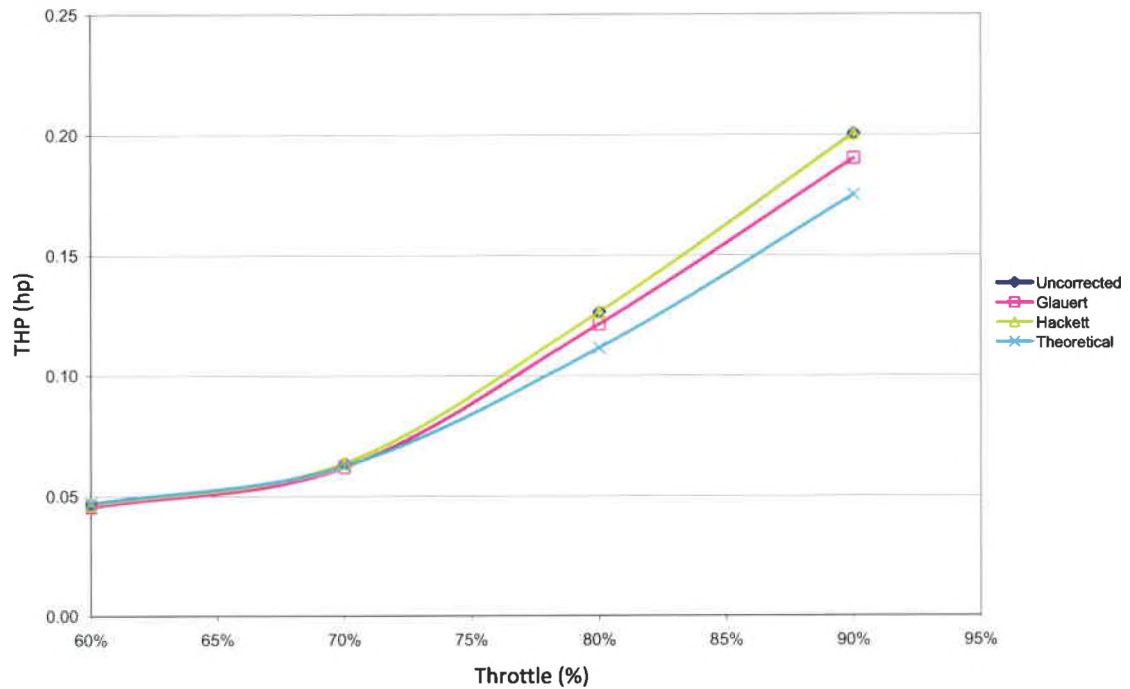


Figure 27 - B40-10S Thrust Horsepower Comparison at 20 mph

Efficiencies vs Power at 20 mph

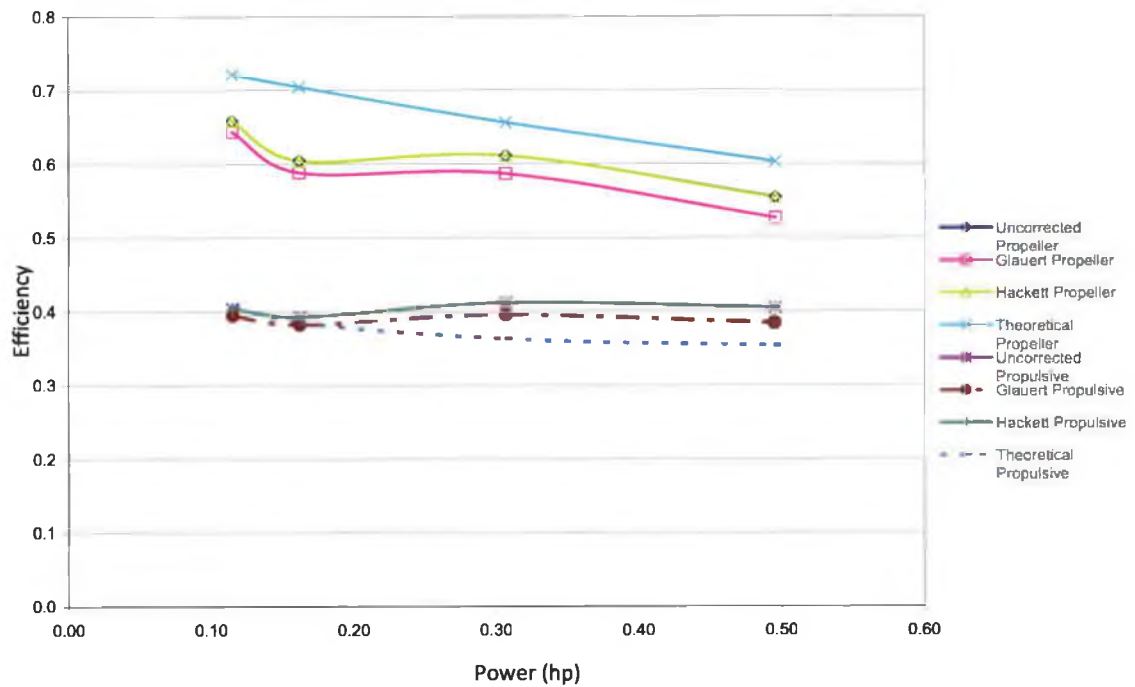


Figure 28 - B40-10S Efficiency Comparison at 20 mph

Just as the case was with the B20-18L at its lowest speed, the B40-10S also needed little correction at 20 mph, its lowest speed. Glauert's method overcorrected the velocity data which can be seen in Figures 27 and 28, with the comparison of THP, Propeller Efficiency, and Propulsive Efficiency respectively. Theoretical data curves can be seen here as they were in the B20-18L 10 mph plots. This data was achieved in the same way using the AFRL momentum-disk theory program to generate each data point for comparison. For this case as well, the theoretical data was reasonably close to the measured curves.

Table 6 - B40-10S Corrected Data at 35 mph

60%				
Metric	Uncorrected	Glauert	Hackett	Theoretical
Ind Velocity (mph)	35.24	34.99	35.24	35.24
Thrust (lb)	0.585	0.585	0.561	0.1877
Torque (lb-ft)	0.0554	0.0554	0.0554	0.034
THP (hp)	0.0550	0.0546	0.0527	0.0176
BHP (hp)	0.0601	0.0601	0.0601	0.0368
Propeller Eff	0.915	0.909	0.877	0.479
Propulsive Eff	0.603	0.598	0.578	0.193
70%				
Metric	Uncorrected	Glauert	Hackett	Theoretical
Ind Velocity (mph)	35.55	35.21	35.55	35.55
Thrust (lb)	0.857	0.857	0.693	0.403
Torque (lb-ft)	0.0807	0.0807	0.0807	0.0526
THP (hp)	0.0812	0.0804	0.0657	0.0382
BHP (hp)	0.0930	0.0930	0.0930	0.0607
Propeller Eff	0.873	0.865	0.706	0.630
Propulsive Eff	0.595	0.590	0.482	0.280
80%				
Metric	Uncorrected	Glauert	Hackett	Theoretical
Ind Velocity (mph)	36.14	35.60	36.14	36.14
Thrust (lb)	1.479	1.479	1.346	0.8925
Torque (lb-ft)	0.1348	0.1348	0.1348	0.0919
THP (hp)	0.1426	0.1405	0.1297	0.0860
BHP (hp)	0.1746	0.1746	0.1746	0.1190
Propeller Eff	0.817	0.805	0.743	0.723
Propulsive Eff	0.576	0.567	0.524	0.347
90%				
Metric	Uncorrected	Glauert	Hackett	Theoretical
Ind Velocity (mph)	36.44	35.58	36.44	36.44
Thrust (lb)	2.735	2.735	2.616	1.8053
Torque (lb-ft)	0.2429	0.2429	0.2429	0.1579
THP (hp)	0.2658	0.2595	0.2542	0.1754
BHP (hp)	0.3656	0.3656	0.3656	0.2377
Propeller Eff	0.727	0.710	0.695	0.738
Propulsive Eff	0.552	0.539	0.528	0.365

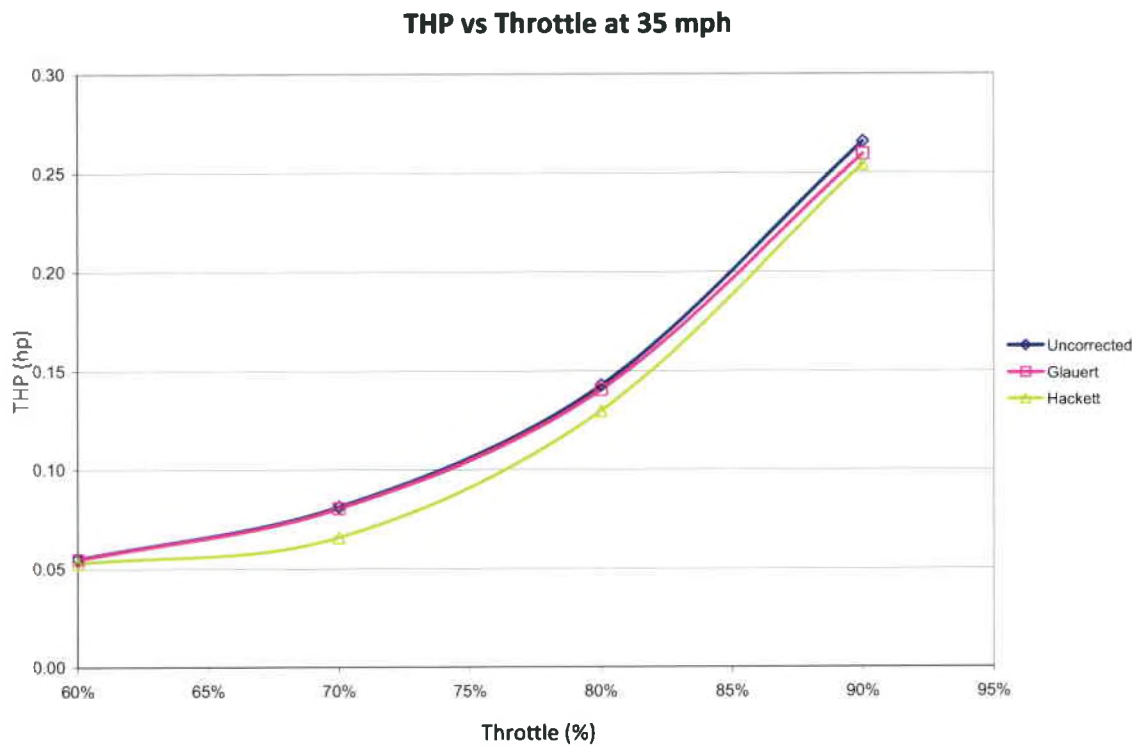


Figure 29 - B40-10S Thrust Horsepower Comparison at 35 mph

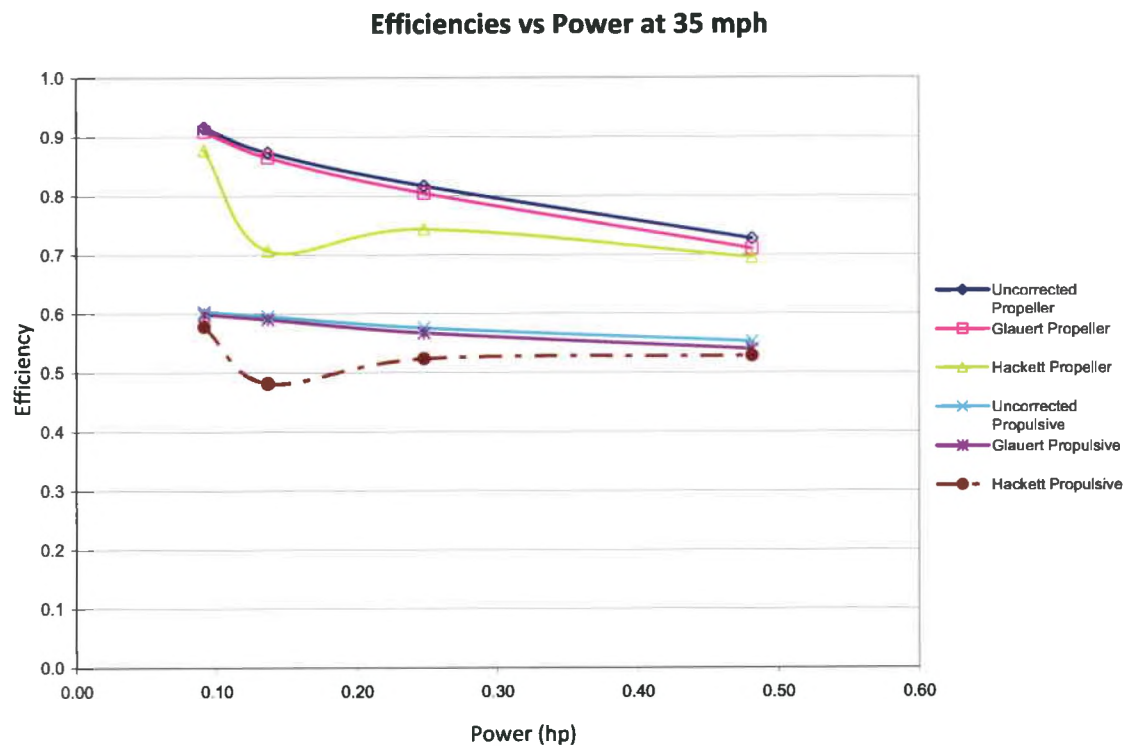


Figure 30 - B40-10S Efficiency Comparison at 35 mph

With a larger propeller on the B40-10S the blockage effect would be expected to happen at an earlier test velocity than the smaller B20-18L, which is exactly what happened. Glauert's velocity correction nearly mirrored the uncorrected measured data as seen in Figures 29 and 30. Hackett's method corrected the data to a larger, more necessary degree than Glauert's. This can be inferred by the uncommonly high propeller efficiency for the measured and Glauert numbers that are both above 90%. With the Hackett correction these 90% efficiencies are reduced to a more plausible level of 87.7%. It is also obvious that the correction the Hackett method applies to the data does not match the curve of the measured data as Glauert's method does. This could be from the fact that Glauert's method shown in Equation 4, calculates its tau variable using the uncorrected thrust which was proven by Hackett's method and other analytical analysis to be inaccurate in most cases. For Glauert's method the thrust stays the same and a percentage of the freestream velocity becomes the velocity that is used to calculate THP and in turn propeller and propulsive efficiency. The unexpected dips in Figures 29 and 30 most likely come from the lack of a clearly defined asymptotic value of the velocity profiles seen in Figures 10-18. In some cases asymptotes can be determined but in most of the cases an educated inference was made. This was the best that could be done with the setup that was available, with only a few downstream pressure tap positions available. The trend of the Hackett corrections is correct as it has little to no correction at the lower speeds and smaller propellers, and much larger corrections at higher speeds and larger propellers. It is the degree of correction that becomes the question based on the given data and setup. If more test section space was available for pressure measurements the assumed asymptotic value seen in Figure 13, effecting Figures 29 and 30, would likely

have been a lot lower, reducing the magnitude of the correction from the Hackett method and eliminating the sudden dip on the Hackett curves. Theoretical curves were not plotted here as the theoretical data differed too much from the measured data.

Table 7 - B40-10S Corrected Data at 50 mph

<u>60%</u>				
<u>Metric</u>	<u>Uncorrected</u>	<u>Glauert</u>	<u>Hackett</u>	<u>Theoretical</u>
Ind Velocity (mph)	50.27	50.12	50.27	50.27
Thrust (lb)	0.482	0.482	0.372	-0.843
Torque (lb-ft)	0.0420	0.0420	0.0420	-0.0503
THP (hp)	0.0646	0.0644	0.0499	-0.1130
BHP (hp)	0.0531	0.0531	0.0531	-0.0635
Propeller Eff	1.217	1.213	0.941	1.780
Propulsive Eff	0.881	0.879	0.681	-1.542
<u>70%</u>				
<u>Metric</u>	<u>Uncorrected</u>	<u>Glauert</u>	<u>Hackett</u>	<u>Theoretical</u>
Ind Velocity (mph)	50.70	50.52	50.70	50.70
Thrust (lb)	0.571	0.571	-0.480	-0.7807
Torque (lb-ft)	0.0517	0.0517	0.0517	-0.0426
THP (hp)	0.0772	0.0769	-0.0649	-0.1056
BHP (hp)	0.0668	0.0668	0.0668	-0.0551
Propeller Eff	1.155	1.151	-0.972	1.917
Propulsive Eff	0.810	0.807	-0.681	-1.107
<u>80%</u>				
<u>Metric</u>	<u>Uncorrected</u>	<u>Glauert</u>	<u>Hackett</u>	<u>Theoretical</u>
Ind Velocity (mph)	50.91	50.61	50.91	50.91
Thrust (lb)	1.029	1.029	-0.168	-0.3146
Torque (lb-ft)	0.0990	0.0990	0.0990	0.006
THP (hp)	0.1397	0.1388	-0.0228	-0.0427
BHP (hp)	0.1398	0.1398	0.1398	0.0085
Propeller Eff	0.999	0.993	-0.163	-5.041
Propulsive Eff	0.747	0.743	-0.122	-0.228
<u>90%</u>				
<u>Metric</u>	<u>Uncorrected</u>	<u>Glauert</u>	<u>Hackett</u>	<u>Theoretical</u>
Ind Velocity (mph)	50.94	50.41	50.94	50.94
Thrust (lb)	1.916	1.916	1.319	0.4071
Torque (lb-ft)	0.1865	0.1865	0.1865	0.0724
THP (hp)	0.2603	0.2576	0.1792	0.0553
BHP (hp)	0.2927	0.2927	0.2927	0.1136
Propeller Eff	0.889	0.880	0.612	0.487
Propulsive Eff	0.708	0.701	0.488	0.150

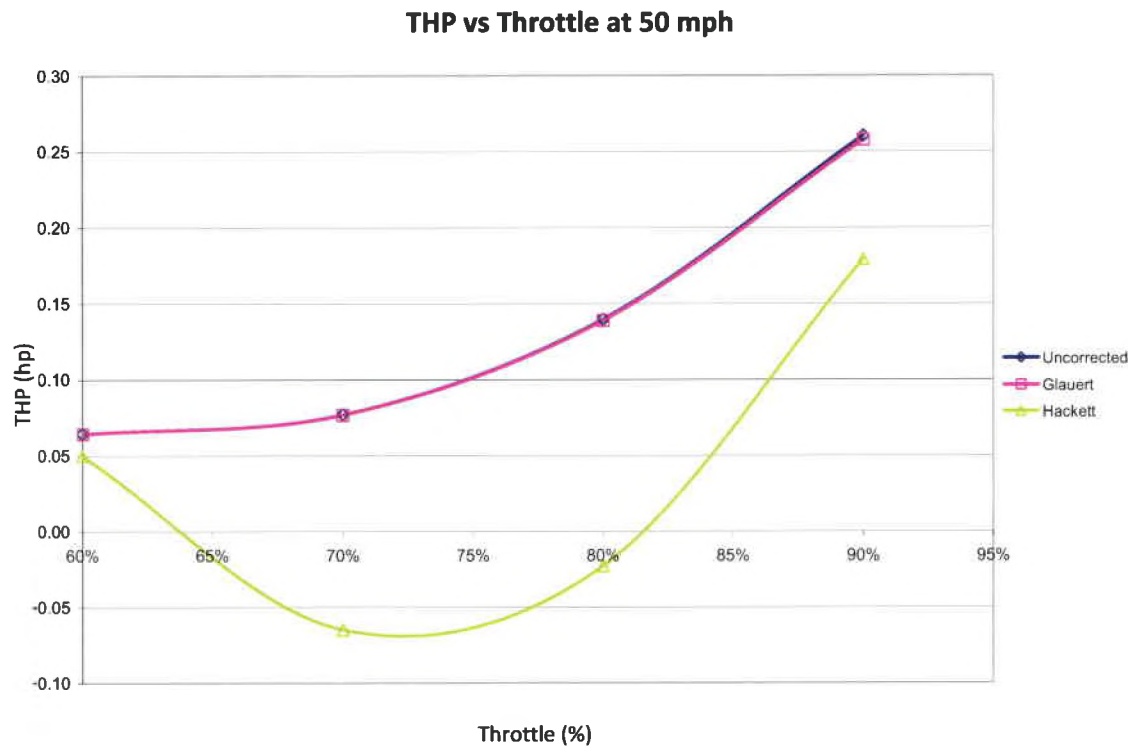


Figure 31 - B40-10S Thrust Horsepower Comparison at 50 mph

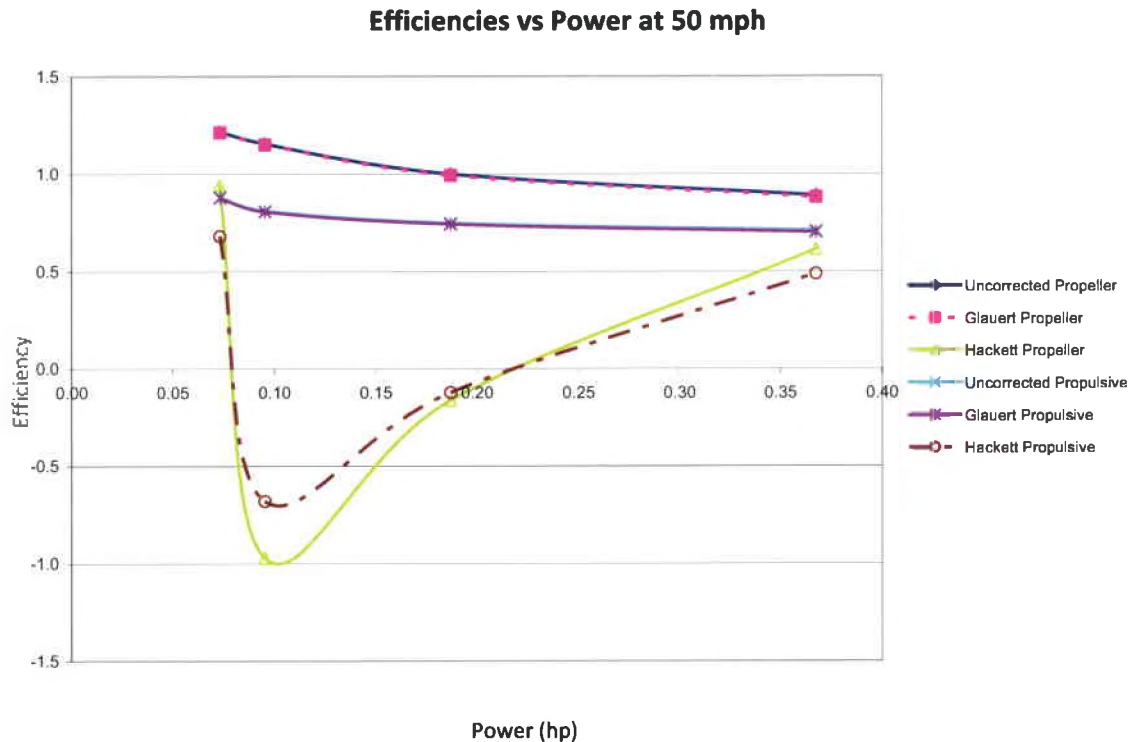


Figure 32 - B40-10S Efficiency Comparison at 50 mph

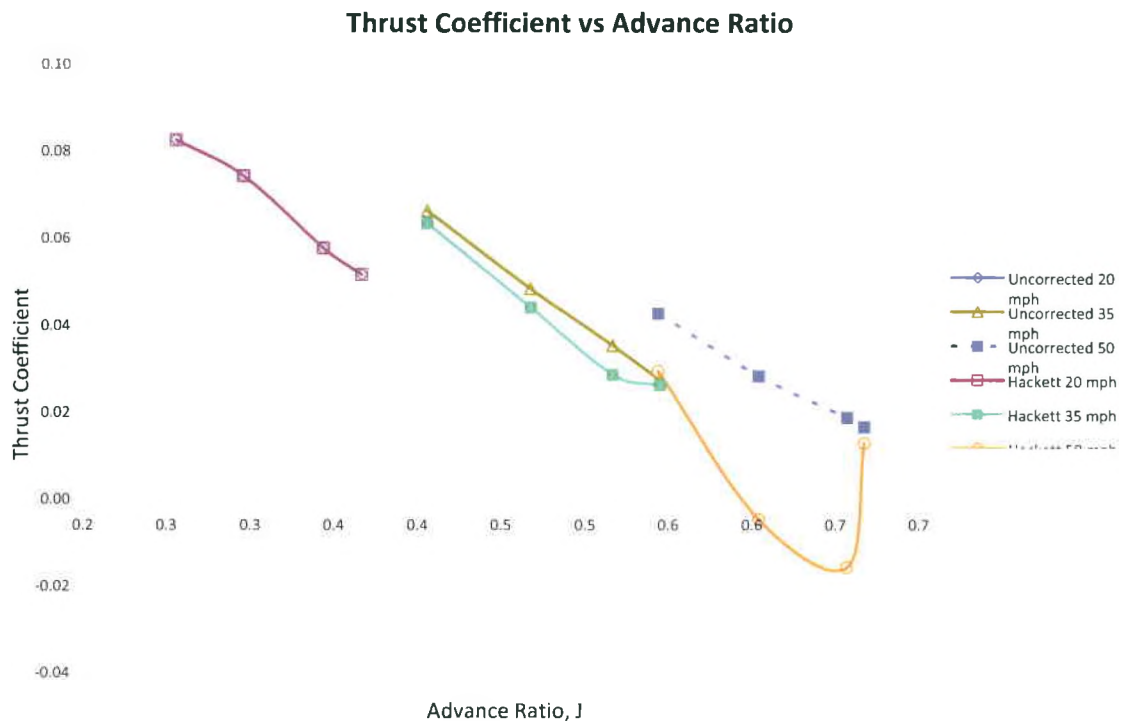


Figure 33 - B40-10S Thrust Coefficient vs Advance Ratio Plot

The same drop in efficiency described for the behavior of the B40-10S at 35 mph, can be seen above in Figure 32 for the same motor at 50 mph. The same performance occurs at the 70, 80, and 90 percent power levels, just to a more pronounced degree which would be expected at a high wind tunnel velocity where larger corrections would be needed. As

discussed above, part of the error could also be from the lack of a defined $\left(\frac{\Delta u}{U_{\infty}}\right)_{MIN}$ value

to calculate the drag corrections with. Had more pressure taps been placed farther downstream of the disk plane, lower asymptotes would have been measured reducing the correction magnitude. Again, the trend is proven with little correction at low velocities and small propeller diameters, and more correction at higher speeds and larger propeller diameters. It is the degree of correction that is in question.

A dimensionless thrust coefficient as a function of advance ratio can also be seen in Figure 33 for all of the B40-10S operating speeds. The uncorrected and Hackett correction curves closely follow each other until an advance ratio of about 0.6 where it diverges greatly. The same explanation for the previous drops in THP and efficiency on the B40-10S motor, can be offered here for the B40-10L. This must be from an overcorrection at the 3rd and 4th data points in Figures 31-33. If not for this the data would be reasonably close to the uncorrected data's trend. Again, the theoretical results were not plotted as they did not match the recorded data enough to be reported on the same plot.

B40-10L

Table 8 - B40-10L Corrected Data at 25 mph

60%				
Metric	Uncorrected	Glauert	Hackett	Theoretical
Ind Velocity (mph)	26.19	25.80	26.19	26.19
Thrust (lb)	0.740	0.740	0.736	0.5163
Torque (lb-ft)	0.0881	0.0881	0.0881	0.0664
THP (hp)	0.0517	0.0509	0.0514	0.0361
BHP (hp)	0.0600	0.0600	0.0600	0.0452
Propeller Eff	0.8610	0.8481	0.8564	0.798
Propulsive Eff	0.5344	0.5264	0.5316	0.373
70%				
Metric	Uncorrected	Glauert	Hackett	Theoretical
Ind Velocity (mph)	26.99	26.44	26.99	26.99
Thrust (lb)	1.149	1.149	1.145	0.8763
Torque (lb-ft)	0.1295	0.1295	0.1295	0.1016
THP (hp)	0.0827	0.0810	0.0824	0.0631
BHP (hp)	0.1000	0.1000	0.1000	0.0784
Propeller Eff	0.8273	0.8103	0.8243	0.804
Propulsive Eff	0.5454	0.5341	0.5434	0.416
80%				
Metric	Uncorrected	Glauert	Hackett	Theoretical
Ind Velocity (mph)	27.01	26.23	27.01	27.01
Thrust (lb)	1.765	1.765	1.761	1.5133
Torque (lb-ft)	0.1909	0.1909	0.1909	0.1569
THP (hp)	0.1271	0.1235	0.1268	0.1090
BHP (hp)	0.1703	0.1703	0.1703	0.1400
Propeller Eff	0.7464	0.7249	0.7446	0.779
Propulsive Eff	0.5252	0.5101	0.5239	0.450
90%				
Metric	Uncorrected	Glauert	Hackett	Theoretical
Ind Velocity (mph)	27.78	26.58	27.78	27.78
Thrust (lb)	3.268	3.268	3.263	2.7696
Torque (lb-ft)	0.3254	0.3254	0.3254	0.2586
THP (hp)	0.2421	0.2317	0.2418	0.2052
BHP (hp)	0.3576	0.3576	0.3576	0.2842
Propeller Eff	0.6770	0.6478	0.6760	0.722
Propulsive Eff	0.5219	0.4994	0.5211	0.442

THP vs Throttle at 25 mph

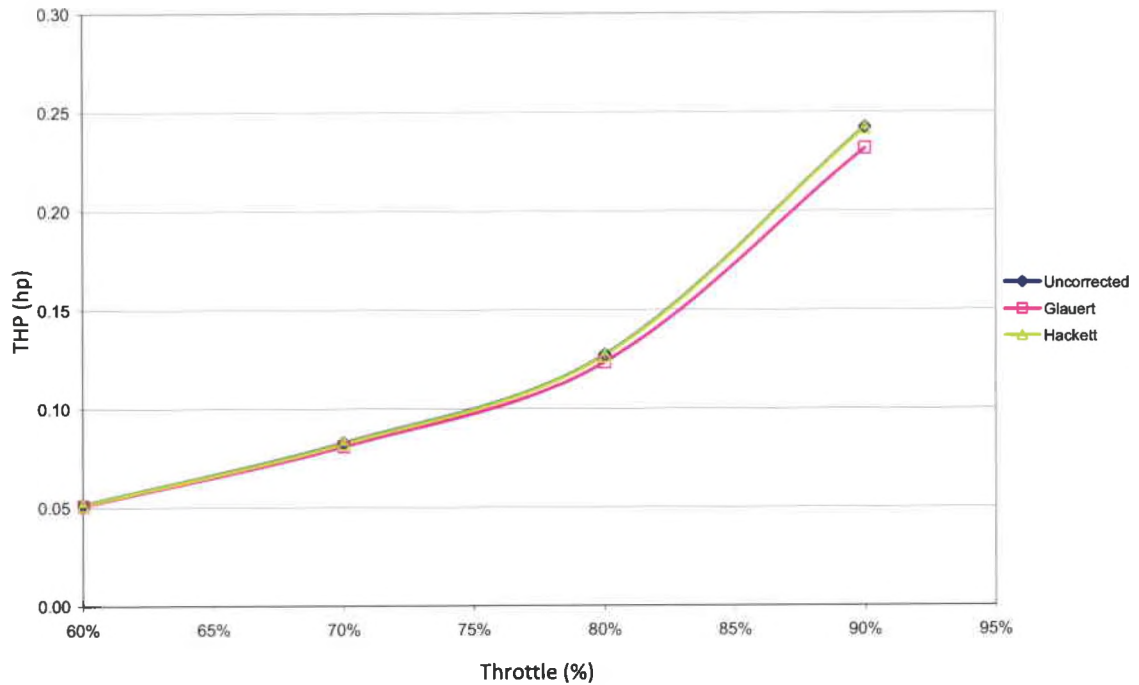


Figure 34 - B40-10L Thrust Horsepower Comparison at 25 mph

Efficiencies vs Power at 25 mph

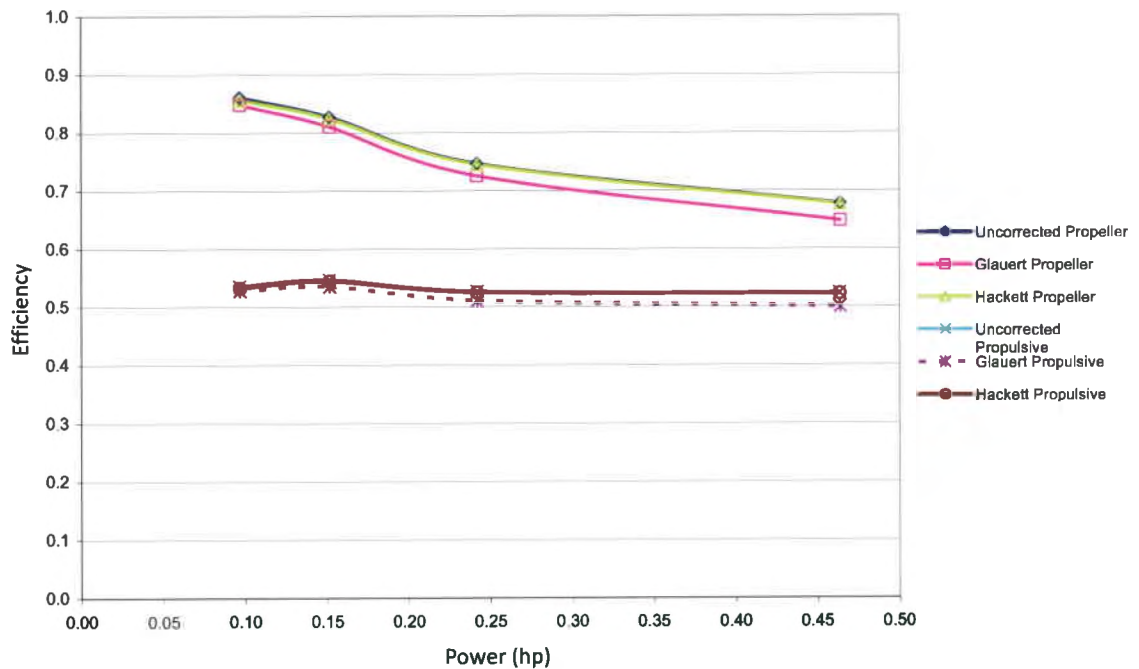


Figure 35 - B40-10L Efficiency Comparison at 25 mph

The B40-10L shows some of the same correction trends as the previous two motors with the Glauert correction correcting more at the lower wind tunnel speeds than the higher speeds, where the correction is more necessary. The three cases closely match each other in THP and propeller efficiency plots seen in Figures 34 and 35 respectively, but differ more so in the propulsive efficiency also seen in Figure 35. Again the Glauert method over corrected the data at the low wind tunnel speeds. Theoretical curves were not close enough to the recorded data for the B40-10L, and will not be seen on any of the remaining plots.

Table 9 - B40-10L Corrected Data at 40 mph

<u>60%</u>				
<u>Metric</u>	<u>Uncorrected</u>	<u>Glauert</u>	<u>Hackett</u>	<u>Theoretical</u>
Ind Velocity (mph)	40.36	40.17	40.36	40.36
Thrust (lb)	0.499	0.499	0.389	-0.1613
Torque (lb-ft)	0.0635	0.0635	0.0635	0.0022
THP (hp)	0.0537	0.0534	0.0419	-0.0174
BHP (hp)	0.0517	0.0517	0.0517	0.0018
Propeller Eff	1.038	1.033	0.809	-9.688
Propulsive Eff	0.700	0.696	0.545	-0.226
<u>70%</u>				
<u>Metric</u>	<u>Uncorrected</u>	<u>Glauert</u>	<u>Hackett</u>	<u>Theoretical</u>
Ind Velocity (mph)	40.89	40.60	40.89	40.89
Thrust (lb)	0.771	0.771	0.668	0.1104
Torque (lb-ft)	0.0959	0.0959	0.0959	0.0371
THP (hp)	0.0840	0.0834	0.0728	0.0120
BHP (hp)	0.0841	0.0841	0.0841	0.0325
Propeller Eff	1.000	0.993	0.866	0.370
Propulsive Eff	0.700	0.695	0.607	0.100
<u>80%</u>				
<u>Metric</u>	<u>Uncorrected</u>	<u>Glauert</u>	<u>Hackett</u>	<u>Theoretical</u>
Ind Velocity (mph)	40.91	40.47	40.91	40.91
Thrust (lb)	1.245	1.245	1.149	0.5337
Torque (lb-ft)	0.1538	0.1538	0.1538	0.0862
THP (hp)	0.1359	0.1344	0.1254	0.0582
BHP (hp)	0.1461	0.1461	0.1461	0.0819
Propeller Eff	0.930	0.920	0.858	0.711
Propulsive Eff	0.685	0.678	0.632	0.294
<u>90%</u>				
<u>Metric</u>	<u>Uncorrected</u>	<u>Glauert</u>	<u>Hackett</u>	<u>Theoretical</u>
Ind Velocity (mph)	41.41	40.65	41.41	41.41
Thrust (lb)	2.370	2.370	2.281	1.622
Torque (lb-ft)	0.2809	0.2809	0.2809	0.198
THP (hp)	0.2618	0.2569	0.2519	0.1791
BHP (hp)	0.3157	0.3157	0.3157	0.2225
Propeller Eff	0.829	0.814	0.798	0.805
Propulsive Eff	0.669	0.657	0.644	0.458

THP vs Throttle at 40 mph

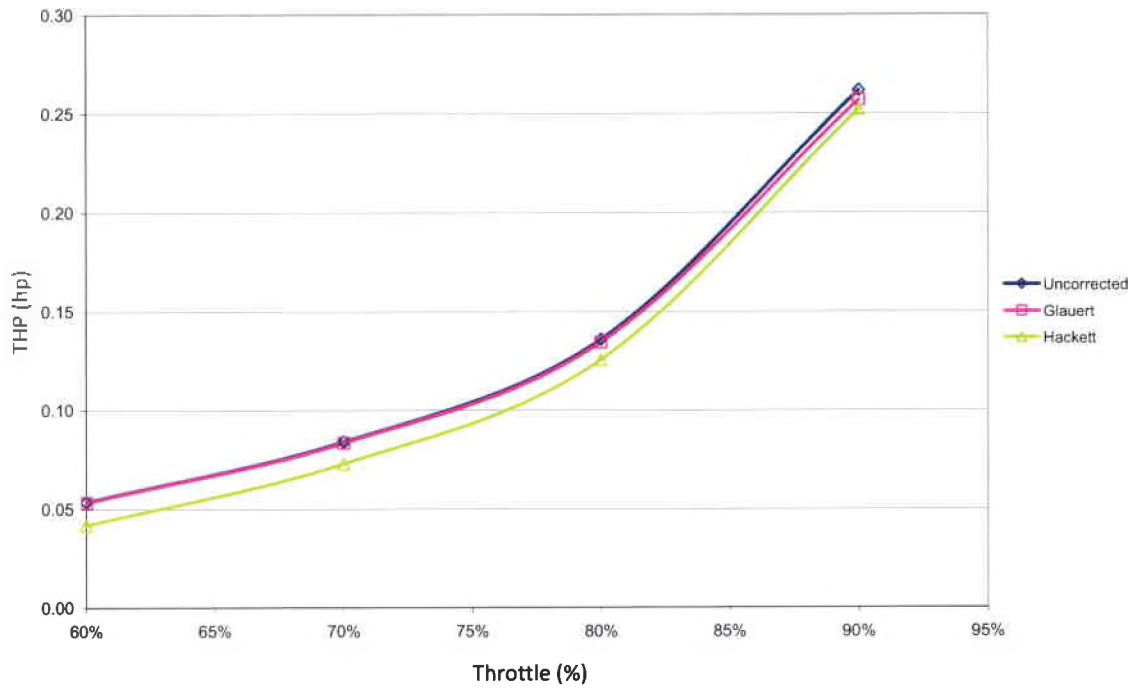


Figure 36 - B40-10L Thrust Horsepower Comparison at 40 mph

Efficiencies vs Power at 40 mph

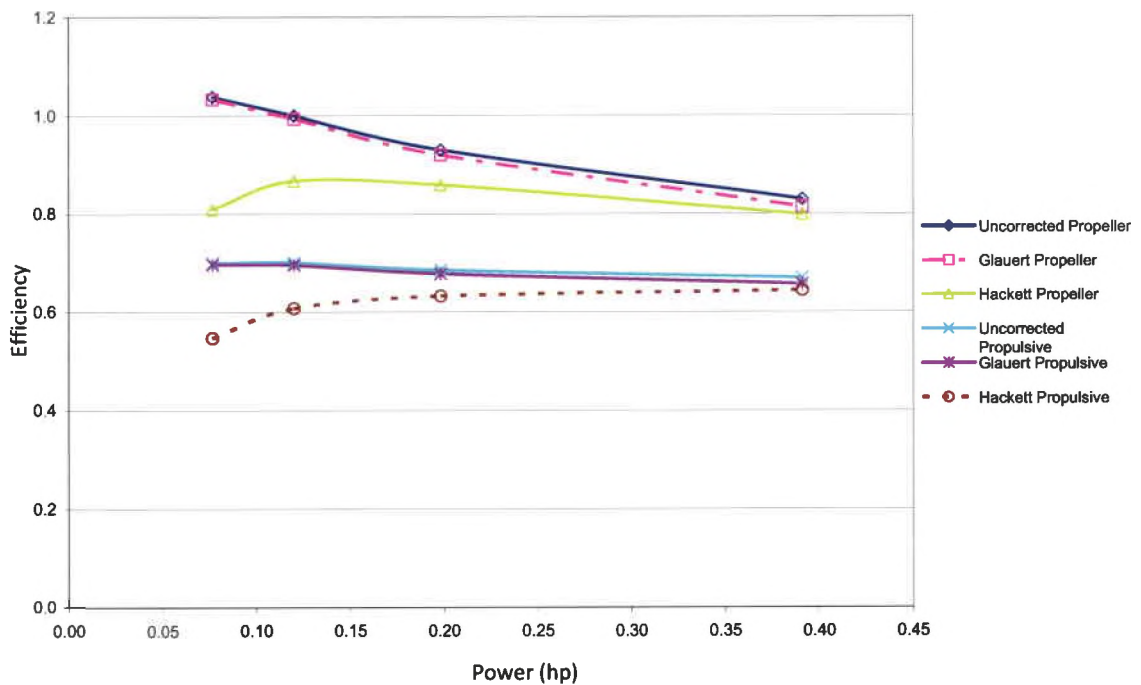


Figure 37 - B40-10L Efficiency Comparison at 40 mph

The largest of the three motors tested was the B40-18L which brought with it a larger propeller and wind tunnel test speeds. This combination of larger propeller and higher test velocities implies that blockage will occur at an earlier test velocity and to a larger magnitude than the B40-10S and especially the B20-18L. Looking at Figure 38, the Glauert correction for THP closely follows that of the measured values with little correction offered at the lower power settings where it would be most needed. The Hackett method, however, corrected the 60% THP case by almost 22% and tapering off to a 4% correction at the 90% THP case, while Glauert only corrected the 60% THP by 0.6% and the 90% THP by 1.9%. Based on the efficiency discrepancies at the lower throttle settings, it seems Glauert corrects more where it is less needed and less where it is more needed.

Table 10 - B40-10L Corrected Data at 55 mph

60%				
<u>Metric</u>	<u>Uncorrected</u>	<u>Glauert</u>	<u>Hackett</u>	<u>Theoretical</u>
Ind Velocity (mph)	55.16	55.06	55.16	55.16
Thrust (lb)	0.341	0.341	-0.481	-1.2443
Torque (lb-ft)	0.0433	0.0433	0.0433	-0.1331
THP (hp)	0.0501	0.0500	-0.0708	-0.1830
BHP (hp)	0.0420	0.0420	0.0420	-0.1291
Propeller Eff	1.193	1.191	-1.685	1.418
Propulsive Eff	0.917	0.915	-1.295	-3.350
70%				
<u>Metric</u>	<u>Uncorrected</u>	<u>Glauert</u>	<u>Hackett</u>	<u>Theoretical</u>
Ind Velocity (mph)	55.55	55.42	55.55	55.55
Thrust (lb)	0.461	0.461	-0.249	-1.0513
Torque (lb-ft)	0.0648	0.0648	0.0648	-0.1017
THP (hp)	0.0683	0.0681	-0.0369	-0.1557
BHP (hp)	0.0654	0.0654	0.0654	-0.1028
Propeller Eff	1.043	1.041	-0.564	1.515
Propulsive Eff	0.842	0.840	-0.455	-1.919
80%				
<u>Metric</u>	<u>Uncorrected</u>	<u>Glauert</u>	<u>Hackett</u>	<u>Theoretical</u>
Ind Velocity (mph)	55.74	55.50	55.74	55.74
Thrust (lb)	0.836	0.836	0.060	-0.6111
Torque (lb-ft)	0.1127	0.1127	0.1127	-0.037
THP (hp)	0.1243	0.1237	0.0090	-0.0908
BHP (hp)	0.1219	0.1219	0.1219	-0.0400
Propeller Eff	1.019	1.015	0.074	2.270
Propulsive Eff	0.844	0.840	0.061	-0.617
90%				
<u>Metric</u>	<u>Uncorrected</u>	<u>Glauert</u>	<u>Hackett</u>	<u>Theoretical</u>
Ind Velocity (mph)	56.13	55.69	56.13	56.13
Thrust (lb)	1.645	1.645	0.794	0.0589
Torque (lb-ft)	0.2108	0.2108	0.2108	0.0516
THP (hp)	0.2461	0.2442	0.1188	0.0088
BHP (hp)	0.2495	0.2495	0.2495	0.0611
Propeller Eff	0.987	0.979	0.476	0.144
Propulsive Eff	0.819	0.812	0.395	0.029

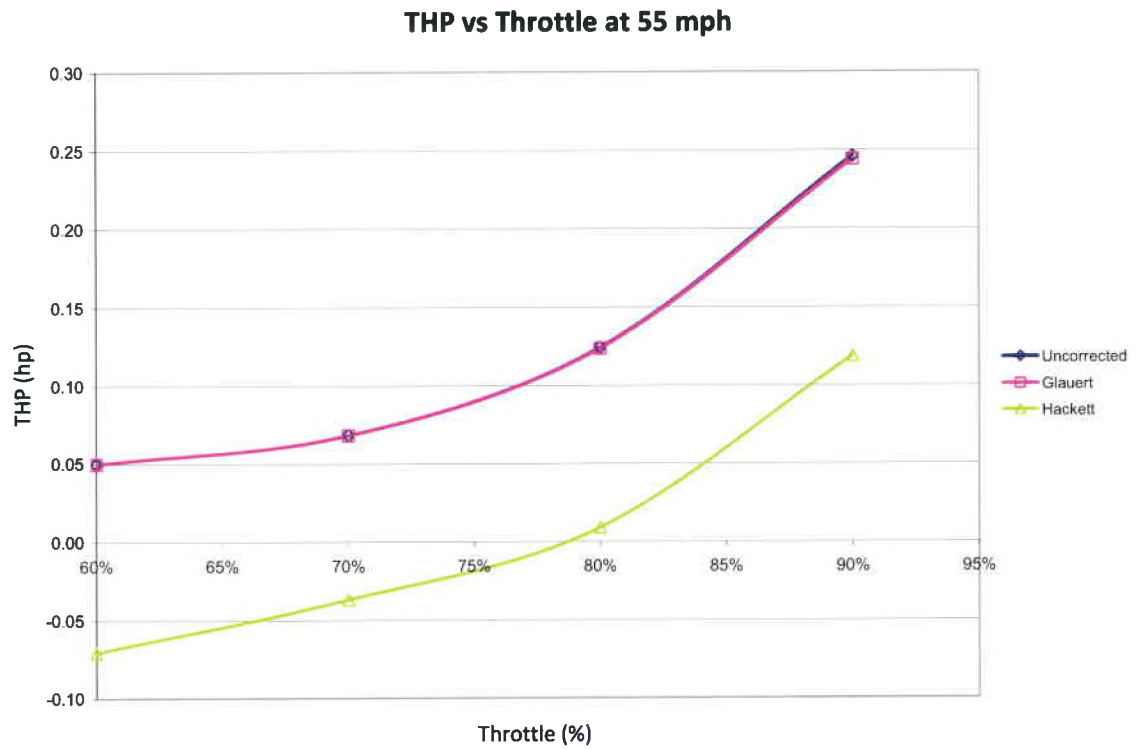


Figure 38 - B40-10L Thrust Horsepower Comparison at 55 mph

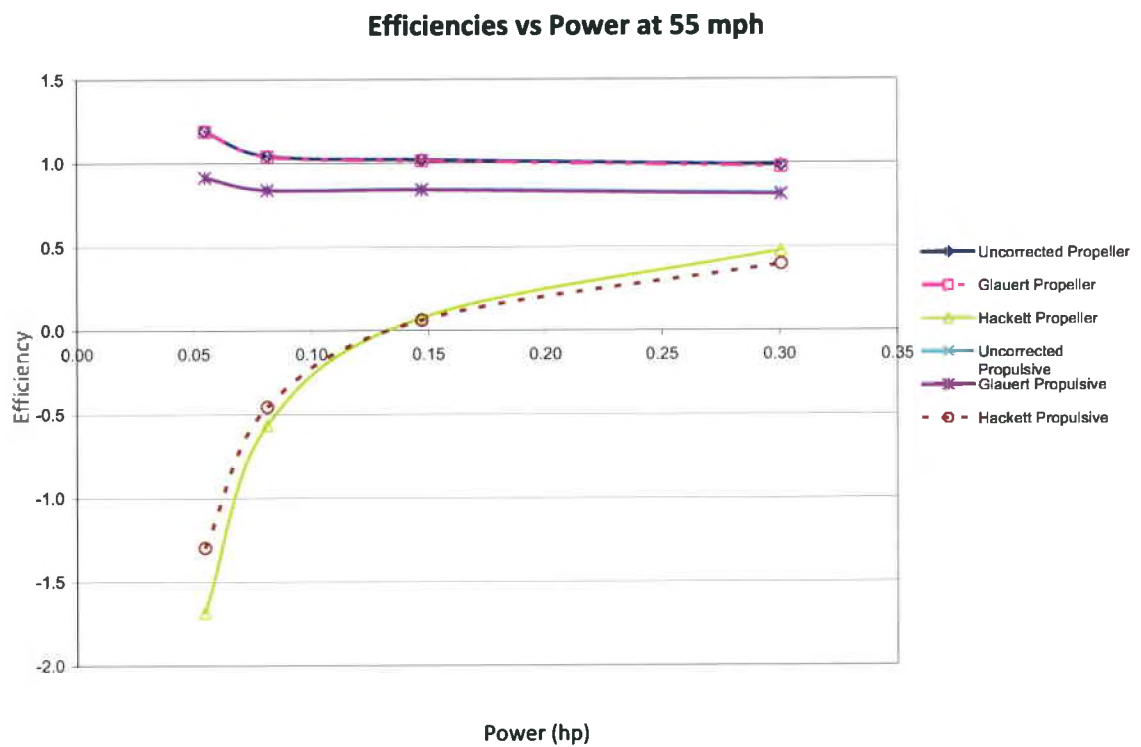


Figure 39 - B40-10L Efficiency Comparison at 55 mph

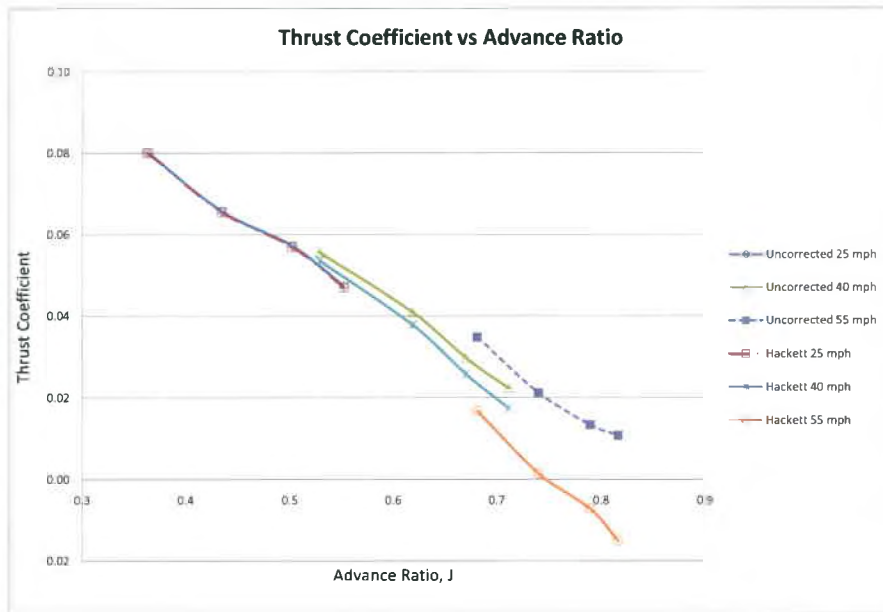


Figure 40 - B40-10L Thrust Coefficient vs Advance Ratio Plot

As previously stated, the trend of the Hackett correction is appropriate with little to no correction at the lower test velocities and larger corrections at the higher wind tunnel speeds where more blockage would logically occur. In the case of the B40-10L at the fastest test speed of 55 mph, it is understandable that the motor at only 60% power would not produce enough thrust to overcome its own drag. This of course would give a negative corrected thrust as the Hackett correction did, corresponding to negative THP, propeller efficiency, and propulsive efficiency. As the power is increased the thrust also increases, improving THP and the two efficiencies until they produce positive thrust at around 80% power. The higher RPMs produced at the 90% power setting pulls more air through the propeller disk plane, decreasing the amount of blockage that occurs requiring less of a correction. This was the case for all of the motors and test runs completed and

was the proven trend. The dimensionless plot for the B40-10L can be seen in Figure 40. The unexpected dips are absent from the B40-10L plots at 55 mph, implying that reasonable asymptotes were estimated to correct the data with the appropriate trend being represented that was discussed earlier.

Experimental Error and Uncertainty

In any experiment there exists a level of error and uncertainty in the data that was recorded. This often is a result of the precision and accuracy of the instruments that were used. Knowing the possible bounds of error for each reading will allow for a calculation of a total error, usually in percentage, for each piece of data that was recorded. The method used in this effort utilized techniques described in Holman's Experimental Methods for Engineers. Since all of the relations being calculated were product functions, the method for calculating uncertainties in product functions was utilized. Given a function of measurement seen in Equation 16

$$R = x_1 x_2 x_3 \quad (16)$$

Where R is a function for an arbitrary performance value that has a level of measurement uncertainty that needs to be calculated, such as THP, BHP, etc., and x_1, x_2 , and x_3 are variables determining R that have a level of uncertainty in their measurement. Partial differentials were then taken of R with respect to each variable, and these partials are then divided by R to get the possible uncertainty of R in percent. This can be seen in Equation 17.

$$\frac{\omega_R}{R} = \left[\left(\frac{\omega_{x_1}}{x_1} \right)^2 + \left(\frac{\omega_{x_2}}{x_2} \right)^2 + \left(\frac{\omega_{x_3}}{x_3} \right)^2 \right]^{1/2} \quad (17)$$

Where ω_R is the uncertainty in R , and ω_{x_i} is the level of uncertainty in each respective variable seen in R . These variable uncertainties are known values based on the instruments used and their respective specifications. The values of x_1 , x_2 , x_3 seen in Equation 17 represent measured values at the same data point R is being calculated at. This presents the possible worst case uncertainty and variance in the data based on the fact that the uncertainty in each of the three variables are given with the same odds. Using this method the uncertainty of the power and efficiencies of the various test runs can be seen in Tables 25-32.

The B20-18L by far had some of the largest possible error percentages. This is due to the fact that the accuracy of the torque cell varied by $\pm .0249$ ft-lbs and some of the torque readings for the B20 were not much larger than this. This error then effected the BHP which subsequently effected the propeller efficiency.

The error dropped dramatically with the increase in motor size and power setting. This is because the outputs of the instruments at these power levels were able to be much larger than the uncertainty of the instruments, allowing for less possible error. For the larger motors and especially the larger motors at the higher power setting the errors reported are much more acceptable.

Motor Comparison

As was stated earlier, the objective of this effort was to enhance the endurance of UAVs through the evaluation of various performance parameters of electric motors. Through this evaluation and comparison it can be seen in which cases and scenarios the most efficient flight could be achieved offering the chance to improve on already mediocre

endurance times. Figures 41-46 compare each of the motor's efficiencies at each of its operating points to the motor closest to it in size based on power. The B20-18L was plotted against the B40-10S, and the B40-10S was plotted against the B40-10L. Each motor was compared against the other based on the low, mid, and high speeds they were tested at.

B20-18L and B40-10S

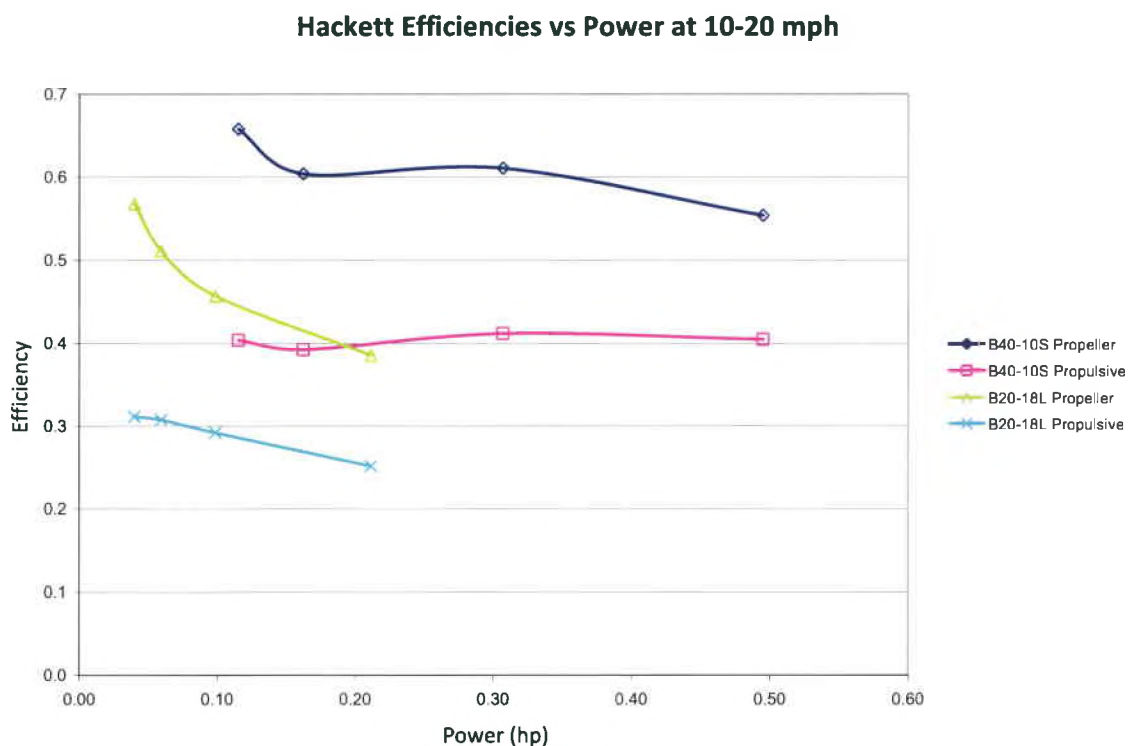


Figure 41 – 10-20 mph B40-10s and B20-18L Efficiency Comparison

Figure 41 shows the low speed comparison of the two smallest motors. For the 10-25 mph scenario the B40-10S was far more efficient than the B20-18L for both propeller and propulsive efficiency, even at the same power setting. The B40-10S is able to cover a

wider power range than the B20-18L at the lower test speed, implying a more flexible motor with a larger flight envelope.

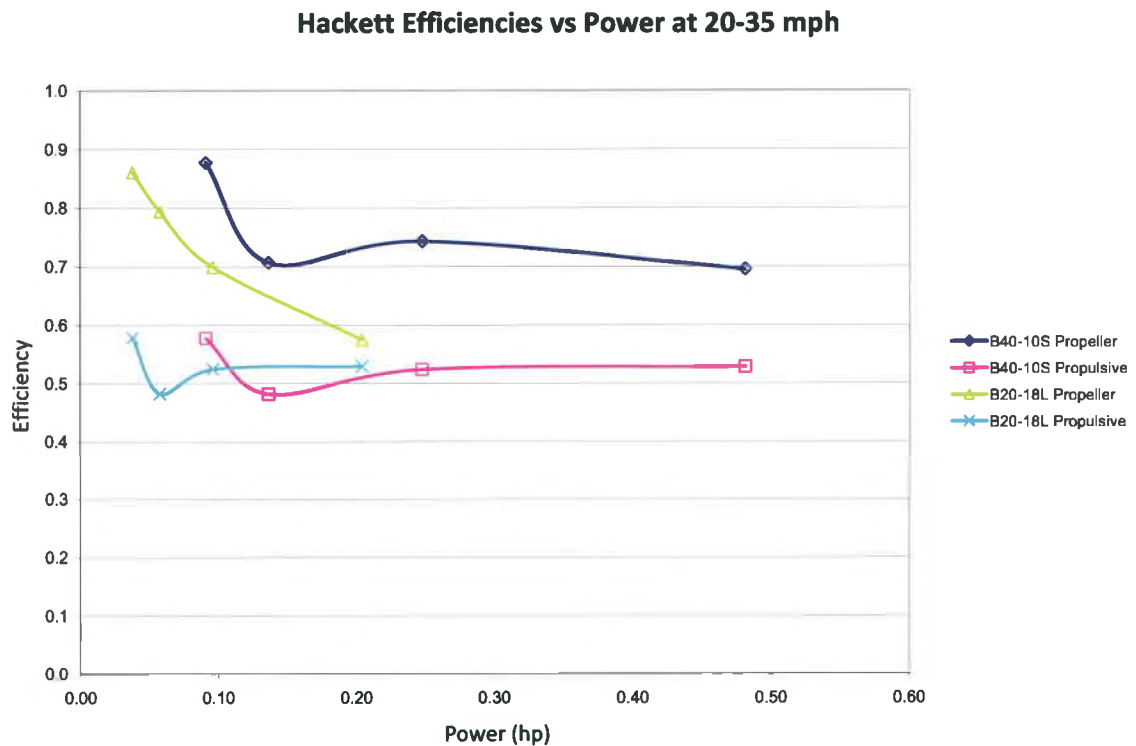


Figure 42 – 20-35 mph B40-10S and B20-18L Efficiency Comparison

At the 20-35 mph velocities for the two motors the B20 is comparable to the B40-10S. The gap in power was narrowed and the B20 is just as efficient and in some cases more efficient than the B40-10S. The B20 is projected by the curve to offer a more efficient propulsion source starting at about 0.10 hp.

Hackett Efficiencies vs Power at 35-50 mph

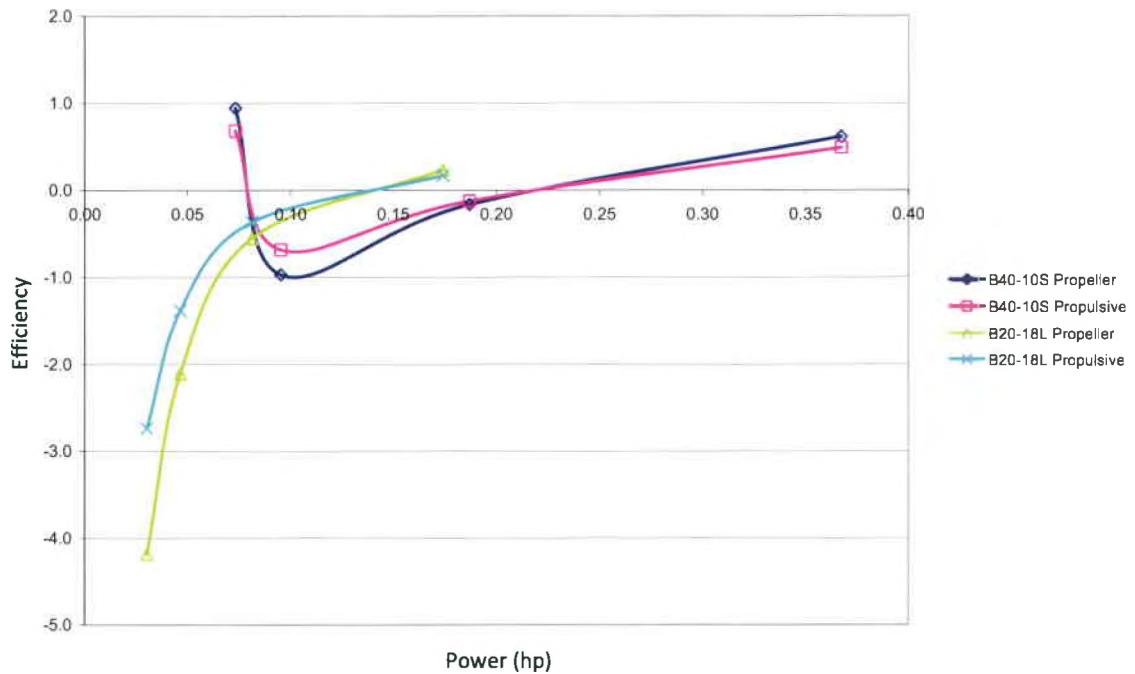


Figure 43 – 35-50 mph B40-10S and B20-18L Efficiency Comparison

At the 35-50 mph velocities for the B20 and the B40-10S the two motors' performance is nearly identical with neither one standing out as the more viable choice for an efficient motor. Also note that the maximum power into the motor at these high velocities has decreased from the two previous plots seen above. This is most likely due to the increased load on the propeller from the freestream.

B40-10S and B40-10L

Hackett Efficiencies vs Power at 20-25 mph

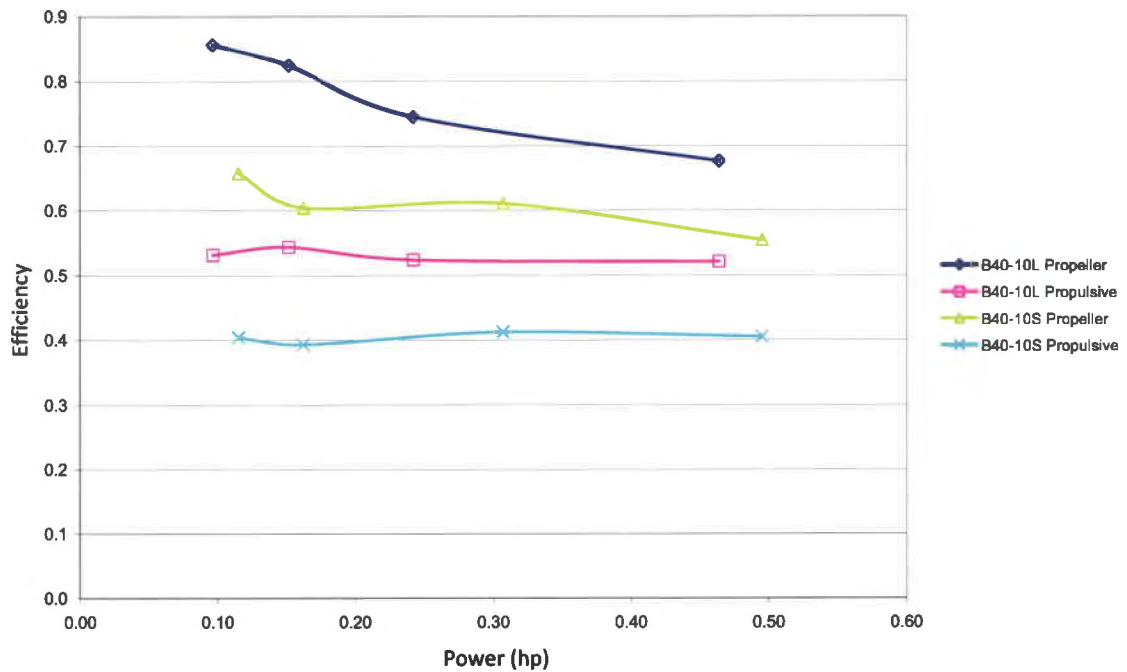


Figure 44 – 20-25 mph B40 Efficiency Comparison

At the 20-25 mph velocities for the B40 motors it is clear that the B40-10L is the more efficient motor capable of greater endurance times. The overall propulsive efficiency for the B40-10L is almost equal to the propeller of the B40-10S, and far greater, by 20% in most cases, than the 10S propulsive efficiency.

Hackett Efficiencies vs Power at 35-40 mph

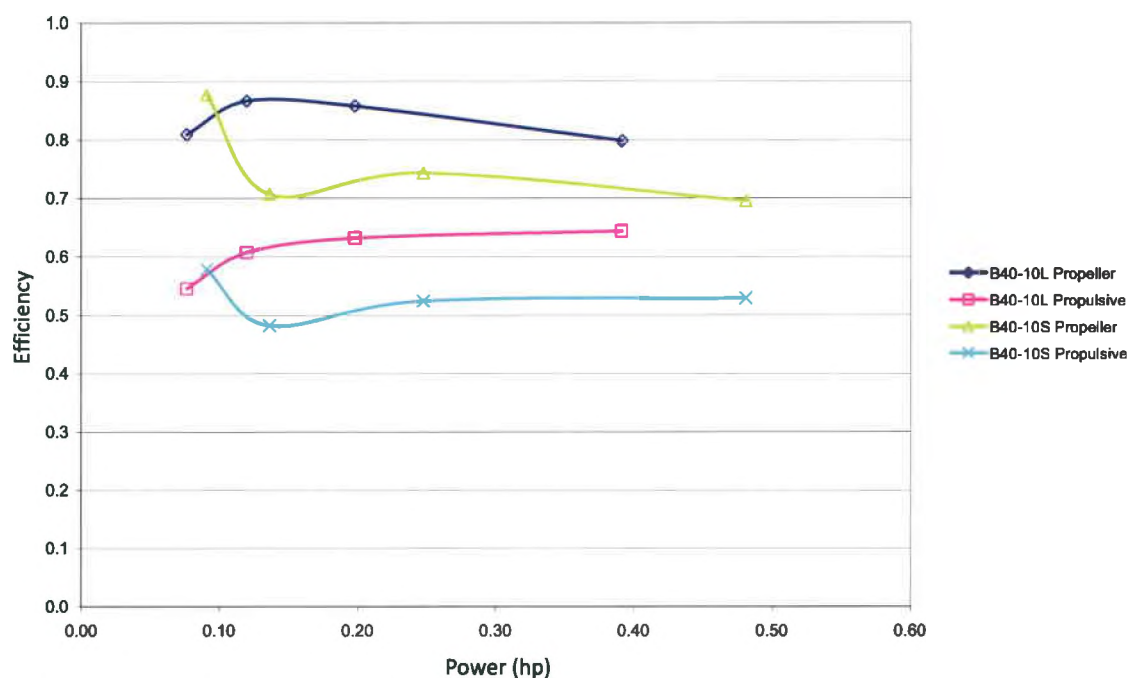


Figure 45 – 35-40 mph B40 Efficiency Comparison

At the 35-40 mph velocities the advantage of the 40L is not as large but is still decisive with a 10% greater efficiency in most cases but not at the lowest power setting. Just below 0.10 hp the B40-10S is more efficient but drops off quickly, making the 10L more efficient at the higher power settings.

Hackett Efficiencies vs Power at 50-55 mph

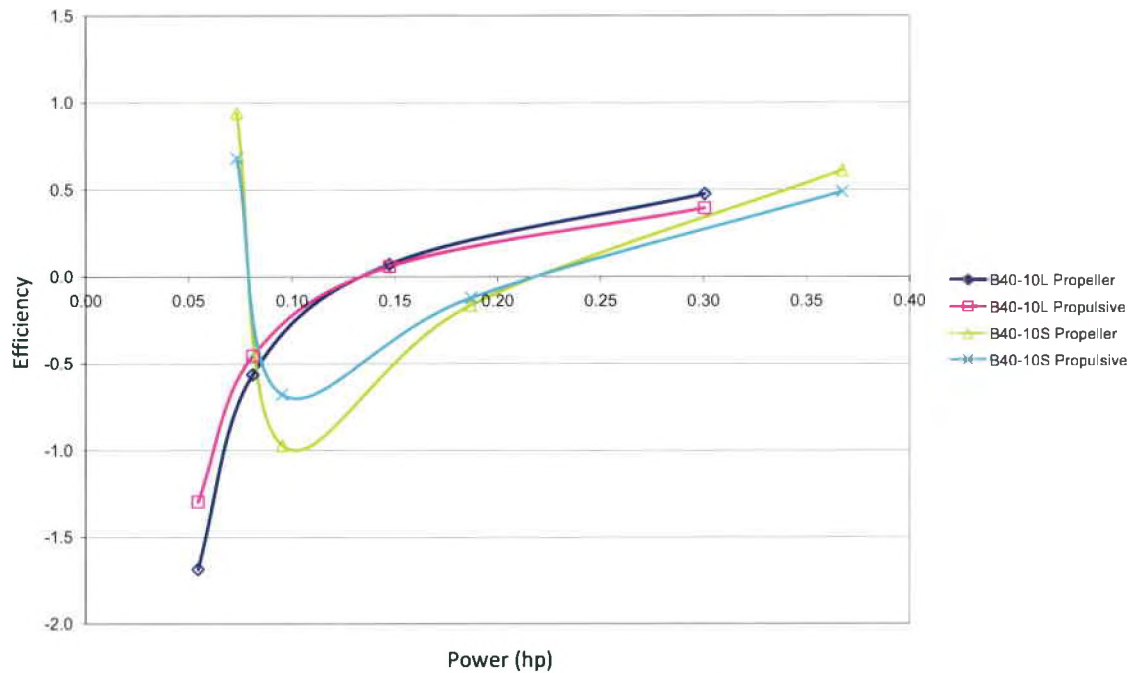


Figure 46 – 50-55 mph B40 Efficiency Comparison

For the 50-55 mph velocity test runs the two motors are very comparable from an efficiency standpoint, as was the case for the previous comparison. Focusing on the more important positive efficiency data points, the B40-10L is slightly more efficient up until about 0.30 hp. This was the maximum power the 10L achieved, but the 10S was able to achieve just over 0.35 hp, and a greater efficiency than the 10L's maximum power level.

Table 11 encapsulates the efficiency information for each motor. It shows each motor's highest THP that it achieved and the corresponding propulsive efficiency along with each motors most efficient operating point and the corresponding THP. It also shows the power to weight ratio of each motor at the reported power for each scenario.

Table 11 - Motor Maximum Power and Efficiency for Corrected Hackett Values

<u>B20-18L</u>		Weight = 0.17 lbs	
<u>Metric</u>	<u>THP (hp)</u>	<u>Power to Weight (hp/lb)</u>	<u>Propulsive Efficiency (%)</u>
Highest Power	0.083	0.488	40.7
Highest Efficiency	0.019	0.112	48.9
<u>B40-10S</u>		Weight = 0.39 lbs	
<u>Metric</u>	<u>THP (hp)</u>	<u>Power to Weight (hp/lb)</u>	<u>Propulsive Efficiency (%)</u>
Highest Power	0.254	0.651	52.8
Highest Efficiency	0.050	0.128	68.1
<u>B40-10L</u>		Weight = 0.47 lbs	
<u>Metric</u>	<u>THP (hp)</u>	<u>Power to Weight (hp/lb)</u>	<u>Propulsive Efficiency (%)</u>
Highest Power	0.252	0.536	64.4
Highest Efficiency	0.252	0.536	64.4

Looking at Table 11, the most efficient motor was the B40-10S but with the second lowest power to weight ratio. With a small sacrifice in efficiency, about 4%, the B40-10L had nearly the same high THP the B40-10S had but was 11.6% more efficient than the B40-10S at that same power. The power to weight ratio of the B40-10L was not quite as high as the B40-10S at the high THP point, but the superior efficiency makes the B40-10L the logical choice for a longer endurance SUAV. Again, the mission profile will also influence which propulsion source to use; this recommendation is based on general performance efficiency with no specific airframe or mission in mind.

CONCLUSIONS

Not even bringing the degree of correction each method produced into context, and first looking at the trend of the correction; it is obvious that the Glauert correction does not properly correct blockages of 8% at higher end velocities, and blockages of 12% and 17% at mid and high end velocities. The inherent problems arise from the fact that the pressure differences between the front and the rear of the disk plane are so great that the thrust is altered by more than the velocity correction can account for in the THP calculation. This subsequently affects the two efficiencies as well. The thrust that goes into the Glauert method is the uncorrected thrust that in most of the higher speed cases were significantly inflated.

The Hackett, Wilsden, and Lilley wall static pressure method more closely followed the appropriate trend of the blockage and corrected to a degree that seemed logical but could not be accurately verified. Hackett's method corrected the slower velocity and smaller propeller runs little to nothing at all, while greatly correcting the higher velocity and larger propeller cases. For all three motors, the wall static pressure corrections offered an avenue to the needed correction to adjust the thrust downward in the cases where there were abnormally high propeller and propulsive efficiencies. The plots of the velocity profiles in Figures 10-18, did not offer hard proof of a sure asymptotic value that could be used to calculate the thrust correction. This brings into question the absolute

magnitude of the Hackett correction but the trend is proven. It would take moving the propeller disk to the front half of the wind tunnel test section, to allow for more distance downstream of the model for an asymptote to appear. This also can be attributed to the large propellers that were used for this size wind tunnel. Smaller propellers would allow for a clearer asymptote as the blockage effect would be less severe than some of the larger propeller cases that were run in this experiment. This can be seen in Figure 10 for the velocity profile of the small B20-18L at its lowest speed of 10 mph. Although the downstream velocity profile is choppy, it definitely starts to even out to form an asymptotic value for $\frac{\Delta u}{U_{\infty}}$ if a trend-line is inserted. This is much harder to see and is not present for the larger motors and higher wind tunnel velocities, even for the B20-18L.

For the cases where there was actually negative thrust, the propeller chosen was not appropriate for that wind tunnel speed and power setting on the motor. Either a lower velocity test run or a larger propeller would be needed to produce enough thrust at lower power settings to avoid the negative thrust, THP, propeller efficiency, and propulsive efficiency. This comes with using a compromise propeller and not a propeller specifically matched to each motor and targeted speed. In short, if the same motor and propellers tested in the wind tunnel were placed on actual UAVs, the aircraft would never reach the airspeeds in steady level cruise that the negative thrusts were recorded at. The real world flight speeds that this experiment was designed around must have been with more high performance propellers.

The University of Maryland paper by Fitzgerald concluded that the Hackett, Wilsden, and Lilley correction was sound. It matched the Glauert method up to a thrust coefficient of 2. The Glauert method was also compared to the Mikkelsen-Sorensen method, which were nearly the same up to a thrust coefficient of 1.2. She used the Glauert method as a baseline comparison for the two more recent methods. The difference between the Maryland effort and this one is the amount of blockage tested and the size of the propellers. Their smallest propeller diameter of 14" was the largest tested here. The blockage area percentages were comparable with what was tested in this effort for the Navy tunnel, but for their larger tunnel, the blockages were much lower than this effort's. Fitzgerald concluded that the Glauert method should be used before any of the new Methods, even Hackett's. This holds true for larger wind tunnels but for smaller ones, like the one used in this effort, that is not the case. In the smaller test section areas seen in this effort, Hackett's method outperforms Glauert's and provided an appropriate correction trend for the data.

Based on the operating conditions evaluated in this effort, it was concluded that the Hackett method was the much needed choice as the trend of the corrections was proven accurate. Under these same conditions the most efficient motor that was tested was the B40-10L. This is only the case when comparing efficiencies and power to weight ratios as was done in the previous section. In reality though, it really depends on the mission and size of the aircraft. As Figures 44-46 show, the operating power level, airspeed, and even propeller choice will dictate the most efficient motor for the mission profile.

FUTURE RESEARCH

There are a few areas where this effort could be extended further. The first would be to verify the magnitude of the Hackett method corrections by using a large enough wind tunnel test section, and placing more static pressure taps downstream of the model so a defined asymptotic value for $\frac{\Delta u}{U_{\infty}}$ can be seen.

Another avenue of development could be to establish a propeller study based off of the motor performance established in this thesis. Numerous propellers can be tested at the same wind tunnel test conditions to see which propeller geometries are required to achieve positive thrust and efficiencies at the faster wind tunnel velocities. Then these same propellers can be evaluated at the lower speeds to see how their efficiencies compare to this study's results. It is expected that propeller geometry will dictate which operating speeds it can efficiently perform at.

Testing could also be initiated on internal combustion engines (ICEs) of similar size to the motors tested in this effort. The Hackett correction method would be applied and the

efficiencies and endurances could be compared based on ranges of assumed airframe $\frac{L}{D}$

and $\frac{W_f}{W_i}$.

APPENDIX A

Table 12 - B20-18L Uncorrected Data at 10 mph

<u>Metric</u>	<u>60%</u>	<u>70%</u>	<u>80%</u>	<u>90%</u>
Volts	9.98	9.97	9.95	9.88
Amps	2.98	4.44	7.41	15.99
Power (W)	29.74	44.27	73.73	157.98
Ind Velocity (mph)	11.36	11.36	11.83	12.62
Ind Velocity Glauert (mph)	11.04	10.95	11.31	11.92
Thrust (lb)	0.409	0.602	0.915	1.586
Torque (lb-ft)	0.0343	0.0489	0.0735	0.1267
RPM	3347	3830	4507	5726
THP (hp)	0.0124	0.0176	0.0289	0.0534
BHP (hp)	0.0218	0.0357	0.0631	0.1382
Propeller Efficiency	0.568	0.512	0.458	0.386
Propulsive Efficiency	0.311	0.307	0.292	0.252
Advance Ratio	0.3584	0.3132	0.2772	0.2327

Table 13 - B20-18L at 20 mph

<u>Metric</u>	<u>60%</u>	<u>70%</u>	<u>80%</u>	<u>90%</u>
Volts	9.98	9.97	9.95	9.88
Amps	2.85	4.32	7.22	15.43
Power (W)	28.44	43.07	71.84	152.45
Ind Velocity (mph)	20.48	20.74	21	21.46
Ind Velocity Glauert (mph)	20.26	20.45	20.61	20.86
Thrust (lb)	0.347	0.499	0.774	1.455
Torque (lb-ft)	0.0321	0.0448	0.0688	0.1317
RPM	3549	4025	4716	5769
THP (hp)	0.0188	0.0272	0.0425	0.0809
BHP (hp)	0.0217	0.0344	0.0618	0.1447
Propeller Efficiency	0.866	0.792	0.688	0.559
Propulsive Efficiency	0.493	0.471	0.442	0.396
Advance Ratio	0.6094	0.5441	0.4702	0.3928

Table 14 - B20-18L at 35 mph

<u>Metric</u>	<u>60%</u>	<u>70%</u>	<u>80%</u>	<u>90%</u>
Volts	9.99	9.98	9.96	9.90
Amps	2.26	3.48	6.09	13.12
Power (W)	22.58	34.73	60.66	129.89
Ind Velocity (mph)	35.33	35.35	35.76	35.63
Ind Velocity Glauert (mph)	35.22	35.20	35.53	35.23
Thrust (lb)	0.268	0.372	0.585	1.115
Torque (lb-ft)	0.0243	0.0352	0.0564	0.1077
RPM	4281	4560	5075	6050
THP (hp)	0.0252	0.0349	0.0554	0.1047
BHP (hp)	0.0198	0.0306	0.0545	0.1241
Propeller Efficiency	1.273	1.141	1.017	0.844
Propulsive Efficiency	0.833	0.749	0.682	0.602
Advance Ratio	0.8715	0.8186	0.7441	0.6219

Table 15 - B40-10S at 20 mph

<u>Metric</u>	<u>60%</u>	<u>70%</u>	<u>80%</u>	<u>90%</u>
Volts	9.94	9.91	9.80	9.68
Amps	8.65	12.21	23.38	38.17
Power (W)	85.98	121.00	229.12	369.49
Ind Velocity (mph)	20.70	21.21	22.19	22.67
Ind Velocity Glauert (mph)	20.23	20.63	21.31	21.52
Thrust (lb)	0.843	1.125	2.136	3.317
Torque (lb-ft)	0.0747	0.1018	0.1647	0.2435
RPM	4971	5433	6602	7802
THP (hp)	0.0455	0.0619	0.1214	0.1903
BHP (hp)	0.0707	0.1053	0.2071	0.3617
Propeller Efficiency	0.643	0.588	0.586	0.526
Propulsive Efficiency	0.395	0.382	0.395	0.384
Advance Ratio	0.3664	0.3435	0.2958	0.2557

Table 16 - B40-10S at 35 mph

<u>Metric</u>	<u>60%</u>	<u>70%</u>	<u>80%</u>	<u>90%</u>
Volts	9.95	9.93	9.86	9.69
Amps	6.84	10.25	18.75	37.05
Power (W)	68.06	101.78	184.88	359.01
Ind Velocity (mph)	35.24	35.55	36.14	36.44
Ind Velocity Glauert (mph)	34.99	35.21	35.60	35.58
Thrust (lb)	0.585	0.857	1.479	2.735
Torque (lb-ft)	0.0554	0.0807	0.1348	0.2429
RPM	5690	6057	6800	7906
THP (hp)	0.0546	0.0804	0.1405	0.2595
BHP (hp)	0.0601	0.0930	0.1746	0.3656
Propeller Efficiency	0.909	0.865	0.805	0.710
Propulsive Efficiency	0.598	0.590	0.567	0.539
Advance Ratio	0.5450	0.5165	0.4677	0.4056

Table 17 - B40-10S at 50 mph

<u>Metric</u>	<u>60%</u>	<u>70%</u>	<u>80%</u>	<u>90%</u>
Volts	9.96	9.95	9.88	9.77
Amps	5.49	7.15	14.12	28.07
Power (W)	54.68	71.14	139.51	274.24
Ind Velocity (mph)	50.27	50.70	50.91	50.94
Ind Velocity Glauert (mph)	50.12	50.52	50.61	50.41
Thrust (lb)	0.482	0.571	1.029	1.916
Torque (lb-ft)	0.0420	0.0517	0.0990	0.1865
RPM	6630	6790	7416	8241
THP (hp)	0.0644	0.0769	0.1388	0.2576
BHP (hp)	0.0531	0.0668	0.1398	0.2927
Propeller Efficiency	1.213	1.151	0.993	0.880
Propulsive Efficiency	0.879	0.807	0.743	0.701
Advance Ratio	0.6672	0.6571	0.6041	0.5440

Table 18 - B40-10L at 25 mph

<u>Metric</u>	<u>60%</u>	<u>70%</u>	<u>80%</u>	<u>90%</u>
Volts	9.95	9.91	9.86	9.70
Amps	7.25	11.42	18.32	35.69
Power (W)	72.14	113.17	180.64	346.19
Ind Velocity (mph)	26.19	26.99	27.01	27.78
Ind Velocity Glauert (mph)	25.80	26.44	26.23	26.58
Thrust (lb)	0.740	1.149	1.765	3.268
Torque (lb-ft)	0.0881	0.1295	0.1909	0.3254
RPM	3576	4053	4686	5772
THP (hp)	0.0509	0.0810	0.1235	0.2317
BHP (hp)	0.0600	0.1000	0.1703	0.3576
Propeller Efficiency	0.848	0.810	0.725	0.648
Propulsive Efficiency	0.526	0.534	0.510	0.499
Advance Ratio	0.5524	0.5023	0.4348	0.3630

Table 19 - B40-10L at 40 mph

<u>Metric</u>	<u>60%</u>	<u>70%</u>	<u>80%</u>	<u>90%</u>
Volts	9.96	9.94	9.88	9.75
Amps	5.75	9.01	14.98	29.95
Power (W)	57.27	89.56	148.00	292.01
Ind Velocity (mph)	40.36	40.89	40.91	41.41
Ind Velocity Glauert (mph)	40.17	40.60	40.47	40.65
Thrust (lb)	0.499	0.771	1.245	2.370
Torque (lb-ft)	0.0635	0.0959	0.1538	0.2809
RPM	4278	4603	4989	5903
THP (hp)	0.0534	0.0834	0.1344	0.2569
BHP (hp)	0.0517	0.0841	0.1461	0.3157
Propeller Efficiency	1.033	0.993	0.920	0.814
Propulsive Efficiency	0.696	0.695	0.678	0.657
Advance Ratio	0.7116	0.6701	0.6185	0.5291

Table 20 - B40-10L at 55 mph

<u>Metric</u>	<u>60%</u>	<u>70%</u>	<u>80%</u>	<u>90%</u>
Volts	9.97	9.96	9.91	9.82
Amps	4.09	6.08	11.09	22.85
Power (W)	40.78	60.56	109.90	224.39
Ind Velocity (mph)	55.16	55.55	55.74	56.13
Ind Velocity Glauert (mph)	55.06	55.42	55.50	55.69
Thrust (lb)	0.341	0.461	0.836	1.645
Torque (lb-ft)	0.0433	0.0648	0.1127	0.2108
RPM	5095	5307	5680	6215
THP (hp)	0.0500	0.0681	0.1237	0.2442
BHP (hp)	0.0420	0.0654	0.1219	0.2495
Propeller Efficiency	1.191	1.041	1.015	0.979
Propulsive Efficiency	0.915	0.840	0.840	0.812
Advance Ratio	0.8166	0.7895	0.7402	0.6812

Table 21 - B20-18L Drag Correction Numbers

B20-18L				
10 mph	A5	Qw	Delta Drag (lbs)	% Change from Uncorrected
60%	0.006	1.250	0.0003	0.07
70%	0.009	1.874	0.0007	0.12
80%	0.015	3.253	0.0020	0.22
90%	0.023	5.206	0.0052	0.33
20 mph	A5	Qw	Delta Drag (lbs)	% Change from Uncorrected
60%	0.015	5.632	0.0060	1.73
70%	0.015	5.513	0.0058	1.16
80%	0.011	4.043	0.0031	0.40
90%	0.012	4.525	0.0039	0.27
35 mph	A5	Qw	Delta Drag (lbs)	% Change from Uncorrected
60%	0.120	77.726	1.1488	428.6
70%	0.115	74.530	1.0562	283.9
80%	0.105	68.838	0.9011	154.0
90%	0.100	65.344	0.8119	72.82

Table 22 - B40-10S Drag Correction Numbers

B40-10S				
20 mph	A5	Qw	Delta Drag (lbs)	% Change from Uncorrected
60%	0.000	0.000	0.0000	0.00
70%	0.003	0.971	0.0002	0.02
80%	0.003	1.017	0.0002	0.01
90%	0.010	3.948	0.0030	0.09
35 mph	A5	Qw	Delta Drag (lbs)	% Change from Uncorrected
60%	0.018	11.306	0.0243	4.15
70%	0.045	29.329	0.1636	19.09
80%	0.040	26.503	0.1336	9.03
90%	0.038	25.052	0.1193	4.36
50 mph	A5	Qw	Delta Drag (lbs)	% Change from Uncorrected
60%	0.026	23.962	0.1092	22.66
70%	0.080	74.360	1.0514	184.1
80%	0.085	79.335	1.1968	116.3
90%	0.060	56.034	0.5970	31.16

Table 23 - B40-10L Drag Correction Numbers

B40-10L				
25 mph	A5	Qw	Delta Drag (lbs)	% Change from Uncorrected
60%	0.010	4.561	0.0040	0.54
70%	0.010	4.701	0.0042	0.37
80%	0.010	4.704	0.0042	0.24
90%	0.010	5.093	0.0049	0.15
40 mph	A5	Qw	Delta Drag (lbs)	% Change from Uncorrected
60%	0.033	24.048	0.1100	22.04
70%	0.031	23.239	0.1027	13.32
80%	0.030	22.500	0.0963	7.73
90%	0.029	21.637	0.0890	3.76
55 mph	A5	Qw	Delta Drag (lbs)	% Change from Uncorrected
60%	0.065	65.732	0.8216	240.9
70%	0.060	61.105	0.7100	154.0
80%	0.063	63.869	0.7757	92.79
90%	0.065	66.888	0.8507	51.71

Table 24 - Pressure Tap Locations in Test Section

Tap Number	B20 Location (in)	B40 Location (in)
1	50.63	48.19
2	38.13	35.69
3	31.63	29.19
4	25.13	22.69
5	12.13	9.69
6	5.56	3.13
7	-1.00	-3.44
8	-6.75	-9.19
9	-13.25	-15.69
10	-20.38	-22.81
11	-26.88	-29.31
12	-33.38	-35.81
13	-39.88	-42.31

Table 25 - B20-18L Error at 10 mph

<u>Value</u>	<u>60%</u>	<u>70%</u>	<u>80%</u>	<u>90%</u>
THP Error	0.203	0.190	0.176	0.161
BHP Error	0.727	0.509	0.339	0.196
Propeller Eff Error	0.755	0.543	0.382	0.254
Power Error	0.001	0.001	0.001	0.001
Propulsive Eff Error	0.203	0.190	0.176	0.161

Table 26 - B20-18L Error at 20 mph

<u>Value</u>	<u>60%</u>	<u>70%</u>	<u>80%</u>	<u>90%</u>
THP Error	0.154	0.127	0.109	0.098
BHP Error	0.776	0.555	0.362	0.189
Propeller Eff Error	0.791	0.570	0.378	0.213
Power Error	0.001	0.001	0.001	0.001
Propulsive Eff Error	0.154	0.127	0.109	0.098

Table 27 - B20-18L Error at 35 mph

<u>Value</u>	<u>60%</u>	<u>70%</u>	<u>80%</u>	<u>90%</u>
THP Error	0.163	0.124	0.090	0.067
BHP Error	1.025	0.708	0.442	0.231
Propeller Eff Error	1.038	0.718	0.451	0.241
Power Error	0.001	0.001	0.001	0.001
Propulsive Eff Error	0.163	0.124	0.090	0.067

Table 28 - B40-10S Error at 20 mph

<u>Value</u>	<u>60%</u>	<u>70%</u>	<u>80%</u>	<u>90%</u>
THP Error	0.109	0.102	0.093	0.090
BHP Error	0.335	0.246	0.152	0.103
Propeller Eff Error	0.352	0.266	0.178	0.136
Power Error	0.001	0.001	0.001	0.001
Propulsive Eff Error	0.109	0.102	0.093	0.090

Table 29 - B40-10S Error at 35 mph

<u>Value</u>	<u>60%</u>	<u>70%</u>	<u>80%</u>	<u>90%</u>
THP Error	0.090	0.074	0.062	0.057
BHP Error	0.451	0.310	0.185	0.103
Propeller Eff Error	0.460	0.319	0.196	0.118
Power Error	0.001	0.001	0.001	0.001
Propulsive Eff Error	0.090	0.074	0.062	0.057

Table 30 - B40-10S Error at 50 mph

<u>Value</u>	<u>60%</u>	<u>70%</u>	<u>80%</u>	<u>90%</u>
THP Error	0.094	0.082	0.056	0.045
BHP Error	0.595	0.484	0.252	0.134
Propeller Eff Error	0.602	0.491	0.259	0.141
Power Error	0.001	0.001	0.001	0.001
Propulsive Eff Error	0.094	0.082	0.056	0.045

Table 31 - B40-10L Error at 25 mph

<u>Value</u>	<u>60%</u>	<u>70%</u>	<u>80%</u>	<u>90%</u>
THP Error	0.095	0.083	0.078	0.073
BHP Error	0.284	0.193	0.131	0.077
Propeller Eff Error	0.299	0.210	0.152	0.106
Power Error	0.001	0.001	0.001	0.001
Propulsive Eff Error	0.095	0.083	0.078	0.073

Table 32 - B40-10L Error at 40 mph

<u>Value</u>	<u>60%</u>	<u>70%</u>	<u>80%</u>	<u>90%</u>
THP Error	0.096	0.072	0.059	0.052
BHP Error	0.394	0.261	0.163	0.089
Propeller Eff Error	0.405	0.271	0.173	0.103
Power Error	0.001	0.001	0.001	0.001
Propulsive Eff Error	0.096	0.072	0.059	0.052

Table 33 - B40-10L Error at 55 mph

<u>Value</u>	<u>60%</u>	<u>70%</u>	<u>80%</u>	<u>90%</u>
THP Error	0.126	0.096	0.061	0.044
BHP Error	0.578	0.386	0.222	0.119
Propeller Eff Error	0.591	0.398	0.230	0.126
Power Error	0.001	0.001	0.001	0.001
Propulsive Eff Error	0.126	0.096	0.061	0.044

BIBLIOGRAPHY

- [1] Glauert, H., The Elements of Airfoil and Airscrew Theory, Cambridge University Press, Cambridge, England, 2nd Edition, 1947
- [2] Shevell, R., Fundamentals of Flight, Prentice Hall, Upper Saddle River, New Jersey 2nd Edition, 1989
- [3] Holman, J.P., Experimental Methods for Engineers, McGraw Hill, New York, New York, 7th Edition, 2001
- [4] Fitzgerald, R., Wind Tunnel Blockage Corrections for Propellers, University of Maryland, College Park, Maryland, 2007